High-index Contrast Grating based Broadband Out-coupler on SOI

Thesis submitted in the partial fulfilment of requirement for the award of degree of

Master of Engineering

in

Electronics and Communication Engineering

Submitted by:

Sunny Chugh

Roll No: 801061026

Under the guidance of:

Dr. Mukesh Kumar

Assistant Professor

ELECTRONICS AND COMMUNICATION ENGINEERING DEPARTMENT

THAPAR UNIVERSITY

(Established under the section 3 of UGC Act, 1956)

PATIALA – 147004 (PUNJAB)

July 2012

DECLARATION

I, Sunny Chugh, hereby certify that the work which is being presented in this thesis entitled "High-index Contrast Grating based Broadband Out-coupler on SOI" by me in partial fulfilment of the requirements for the award of degree of Master of Engineering in Electronics and Communication Engineering from Thapar University (Deemed University), Patiala, is an authentic record of my own work carried out under the supervision of Dr. Mukesh Kumar.

The matter presented in this thesis has not been submitted in any other University / Institute for the award of any other degree.

Date: 3-7-12

Sunny Chugh
Roll No: 801061026

It is certified that the above statement made by the student is correct to the best of my knowledge and belief.

Date: 3/7/12

Dr. Mukesh Kumar
Assistant Professor
ECED

Countersigned by:

(Dr. Rajesh Khanna)
Professor and Head ECED
Thapar University, Patiala
Date:

(Dr. S.K. Mohapatra)
Dean of Academic Affairs
Thapar University, Patiala
Date:

i

ACKNOWLEDGEMENT

I would like to express my special thanks and deep sense of gratitude to my Thesis Adviser, **Dr. Mukesh Kumar,** Assistant Professor, Electronics & Communication Engineering Department, Thapar University, Patiala for their continuous indefatigable guidance which paved me on to the path to carry this thesis within time. I am highly indebted to them for their painstaking efforts and invaluable suggestions during the period of work.

I take this opportunity to express my gratitude and sincere thanks to **Dr. Rajesh Khanna**, Professor and Head , **Dr. Kulbir Singh**, Associate Professor of Electronics & Communication Engineering Department for their valuable advice and suggestion and for providing me the opportunity to complete my thesis work .

I would also like to thank all the staff members of Electronics & Communication Engineering Department for providing me all the facilities required for the completion of this work.

Date: 3-7-12

(Sunny Chugh)

Place: Patiala

ABSTRACT

Coupling structures between an optical fiber and waveguide are fundamental components and have been a standing challenge in integrated optics. In an effort to move this important issue along, this thesis work mainly concentrates on analysis of strong grating couplers. Optical grating has been comprehensively studied over the years due to its diverse applications in holography, spectroscopy, lasers, and many other optoelectronic devices. One of the innovative forms of grating is the High-index contrast grating (HCG). It is possible to control the out-coupled and transmitted light by optimizing the HCG parameters. The recent advances of high-index-contrast (HCG) grating and its applications in optoelectronic devices are reviewed. From application point of view, incoming light can be from another optical chip (inter-chip) or from the same chip (intra-chip).

An efficient broadband out-coupler on Silicon-on-Insulator (SOI) with high-index contrast grating (HCG) is proposed. The presence of a silicon-air (high-index contrast) grating on the top silicon layer in SOI allows a strong interaction between the guided mode and the grating. The design of the out-coupler is presented by optimizing the various grating parameters, grating thickness (t_g), Si thickness (t_{si}), grating period (Λ), duty cycle (C) to obtain the maximum coupling efficiency (η) over a broad range of wavelength (λ). Design and simulation of such an out-coupler is performed with finite difference method. Coupling efficiency of 54% is observed over an ultra-wide wavelength range from 1500nm to 1650nm.Such gratings can also find applications in High Q-resonators. Polarisation insensitivity has been achieved for a wavelength band of 20nm ranging from 1550nm to 1570nm by optimising the grating parameters.

TABLE OF CONTENTS

Declaration **i**

Acknowledgement **ii**

Abstract **iii**

Table of Contents **iv**

List of Figures **vi**

1. Introduction **1**

1.1 Motivation 1

1.2 Couplers – fundamentals and applications 2

1.3 Optical grating couplers 3

1.4 Silicon-on-insulator (SOI) 4

1.5 Purpose and outline of work 4

2. Optical Gratings – Fundamentals and Emerging Trends **5**

2.1 Grating Coupler theory 5

2.1.1 Bragg diffraction 5

2.1.2 Reciprocity 6

2.1.3 Symmetry 6

2.1.4 Positive & Negative detuned gratings 7

2.1.5 Definitions 7

2.2 Grating Couplers 8

2.2.1 Basic grating physics 9

2.3.2 Output Coupling with a Grating Coupler 11

2.3.3 The Coupling coefficient 13

2.3 Coupling to fiber 14

2.3.1 Introduction to coupling 14

2.3.2 Coupling schemes 14

2.3.2.1 Horizontal coupling using tapered waveguides 14

2.3.2.2 Vertical coupling using a grating coupler 15

2.4 SOI Waveguide structures 16
2.4.1 Large single mode waveguides 17
2.4.2 Strip nano waveguides 17
2.5 Emerging trends in SOI grating coupler structures 18
2.5.1 Grating with upper index matching layer 18
2.5.2 Grating with bottom reflector 19
2.5.3 Grating with top mirror 19
2.5.4 Metal gratings 20
2.5.5 Blazed gratings 20
2.5.6 Chirped gratings 21
2.5.7 Gratings with rear reflector 21
2.6 Diffraction Grating Applications 22
3. Literature Survey 24
4. Design and Simulation of Broadband SOI Out-coupler 29
4.1Design of Grating Out-coupler 29
4.1.1 Introduction 29
4.1.2 Structure of basic SOI grating out-coupler 30
4.1.3 Extension with a Gold Bottom Mirror 32
4.2 Simulation Results 33
4.2.1 Effective refractive index 33
4.2.2 Coupling efficiency 33
4.2.3 Coupling efficiency to fiber 37
4.2.3.1 Vertical coupling to fiber 38
4.2.3.2 Coupling to fiber at different angles 39
4.2.4 Coupling efficiency for TE and TM polarisation 40
5. Conclusion 43
References

LIST OF FIGURES

Sr. No.	Figure	Page No.
1.1	Sketch of vertical fiber coupling arrangement	3
2.1	Bragg diffraction on the grating surface	6
2.2	Perfect vertical coupling	6
2.3	Positive and negative detuned gratings	7
2.4	Side view of the grating coupler with design parameters	8
2.5	The incident beam is broken into transmitted, reflected, and diffracted beams, when a grating coupler is illuminated with an incident beam	9
2.6	K-space diagram of a wave diffracting backwards of a grating, the grating subtracts a value K from the z component of the input wavevector	10
2.7	K-space diagram shows a grating on a high-index thin film, placed on a moderate-index substrate. The angle of incidence is exactly right for the grating to couple light into the waveguide	11
2.8	Guided wave incident upon a grating coupling some energy into diffracted waves	12
2.9	Single-beam coupler can be built by making the grating wavenumber so large that the phase-matching condition cannot be met in the cover region. The only coupled power radiates into the substrate	12
2.10	Fiber butt coupling to waveguide	14
2.11	Coupling to fiber using an inverse taper	15
2.12	Coupling to fiber using a grating coupler	16
2.13	SOI wafer structure	16
2.14	Large single mode rib waveguide cross section	17
2.15	Strip nano waveguide cross section	18
2.16	Grating coupler with index matching layer	18
2.17	Grating coupler with bottom mirror	19

2.18	Grating coupler with top mirror	19
2.19	Metal grating coupler	20
2.20	Blazed grating coupler	20
2.21	Chirped grating coupler	21
2.22	Grating coupler with rear reflector	21
4.1	Effective index variations along with the corresponding electric field (E_y) variations at guiding mode	29
4.2	Schematic side-view of Out-coupler on SOI with propagation direction z. t_g is grating thickness with Si thickness as t_{si}.Λ signifies the period of grating	30
4.3	Field propagation in Out-coupler	31
4.4	Field plot of the optimized SOI structure with a gold bottom mirror	32
4.5	Simulation results of coupling efficiency at wavelength, λ=1.55µm for the variations of grating thickness (t_g) with grating period (Λ)	34
4.6	Simulation results of coupling efficiency at wavelength, λ=1.55µm for the variations of grating thickness (t_g) with Si thickness (t_{si})	35
4.7	Effects of duty cycle(C) on coupling efficiency for various values of Λ with parameters λ=1.55µm, t_g =80nm and t_{si}=220nm	36
4.8	Coupling Efficiency (η) of a regular grating broadband SOI coupler for variations in grating period (Λ) & Si thickness (t_{si}) with wavelength (λ) at optimized parameters t_g=80nm, C=0.5, t_{si}=220nm	36
4.9	Comparison between outcoupled power (powerup) with power coupled to fiber at various angles for TE polarisation at λ=1.55µm at t_{si}=220nm,C=0.5, t_g=80nm	37

4.10	Comparison between outcoupled power with power coupled to vertical fiber for TE-polarisation with air on top at Λ=570nm, t_{si}=220nm,C=0.5, t_g=50nm	38
4.11	Comparison between outcoupled power with power coupled to vertical fiber for TE-polarisation with index matching layer (refractive index=1.46) on top at Λ=570nm, t_{si} =220nm, C=0.5, t_g=50nm	39
4.12	Comparison between outcoupled power with power coupled to fiber at different angles of $8^0$and 10^0 for TE-polarisation with air and index matching layer (refractive index=1.46) on top with parameters Λ=610nm,t_{si}=220nm, C=0.5, t_g=50nm, beam diameter of fiber - 12.2µm, align of fiber - 7.1 µm	39
4.13	Variations of outcoupled power efficiency with period for TE and TM polarisations with air on top at λ=1.55µm, t_g=80nm, C=0.5, t_{si}=220nm	40
4.14	Coupling Efficiency (η) of a regular grating broadband SOI coupler for variations in (i) Si thickness (t_{si}) & (ii) grating thickness (t_g) for TE & TM polarisations at optimized parameters C = 0.5, Λ = 800nm, λ = 1.55µm.	41
4.15	Comparison between outcoupled power efficiency with wavelength (λ) for TE & TM polarisation with air on top for optimal parameters Λ=800nm, t_{si}=220nm,C=0.5, t_g=80nm	42

Chapter 1

Introduction

1.1 Motivation

Since their commencement in the 1960s, integrated optical systems have played an important role in advancing and modernizing the telecommunications industry. Within the last decade the free market has invested enormous sums of money into high technology companies specializing in technologies that employ the advances in integrated optical systems.

Currently, high index contrast waveguides are being actively investigated. The desire to migrate to high index contrast devices is driven by one critical factor: the high optical confinement of high index contrast devices waveguides.

Competition in today's telecommunications market in delivering low cost, highly reliable, and high quality telephone, internet, and video service to the office and home is a driving factor in photonic component and PLCs (planer light wave circuits) development. A critical issue associated with their development and implementation is packaging. By far, the most critical aspect of packaging is a precise fiber optic alignment in which PLCs are interfaced with other optical components and devices either by single mode optical fibers or fiber arrays. The difficulty, and challenge, lies in the fact that there is a considerable size differential between the single mode fibers and their interface components, photonic crystals and high index contrast waveguides, which results in a poor mode overlap between them.

Motivations for using optical communication include:

1. Optical communication links have a wider bandwidth than copper or microwave links, so more information can be carried on a given link. The effective bandwidth of current optical fibers is approximately 25 THz.
2. Attenuation in glass fibers is less than experienced in copper or microwave systems. Fewer repeaters are required, and longer distances can be spanned more cost effectively.
3. Optical systems are smaller and lighter, giving them an advantage in crowded ducts or aircraft.
4. Optical waveguides are difficult (but not impossible) to tap or monitor, so data security is higher.

5. Optical waveguides are immune from electromagnetic interference, ground loops, induced cross talk, etc.
6. Finally, and perhaps most important, semiconductor technology has developed a family of lasers, detectors, and other integrated optical devices that are compatible with optical fibers in power, wavelength, and size.

1.2 Couplers - fundamentals and applications

Researchers rapidly discovered that free space propagation of laser beams was not suitable for reliable communication links. Problems of bad weather (precipitation), flying objects that interrupted the beam and the need for line-of-sight links complicated reliable transmissions. A solution to these problems is to propagate light through a waveguide which both protects the beam from interruptions and counters diffraction.

Waveguide/fiber interconnection is a critical feature in the use of Optical waveguide devices. The large dimensional mismatch between common optical single mode fibers and waveguides, and their respective mode sizes, complicates coupling of light from one to the other. The advantages and disadvantages of the most widely used coupling methods are discussed briefly below.

In end-fire coupling, a lens or micro-lens can be used to focus light from a fiber into a waveguide. End-fire coupling is often used in the laboratory because of its convenience. However, the alignment tolerance is tight.
Another method uses lensed fibers. In this method fibers with a tapered section can therefore be used to couple light with greater efficiency into small-core waveguides. This approach is useful for experimental measurements in the laboratory. It does not, however, offer robust and reliable coupling to sub-micron waveguide cores.
A common approach reported in the literature is the use of tapered couplers [1, 2]. An alternative taper technique is to fabricate a second waveguide layer on top of the small size high index contrast waveguide. The top waveguide has a low index contrast and is designed to be single mode with a large core size comparable to the fiber core size. Efficient light coupling first takes place between the incident fiber and this auxiliary waveguide. Then, the light is routed from one layer to the other by means of horizontal and/or vertical tapers of the waveguides in both layers. Tapered couplers are used in commercially available products such as semiconductor lasers and semiconductor optical amplifiers (SOA).The tapered couplers just introduced share a number of challenges. These include (1) generally

complicated processes to fabricate and integrate the tapered structure with other devices; and (2) input/output coupling, I/O, can take place only on the edge.

In these three types of methods, input and output coupling take place only on the edge of a chip at the plane of the waveguide device layer. This edge coupling arrangement severely limits the number of optical I/Os in dense PLCs. Moreover, fiber alignment has to be done after the wafer is diced into separate chips, and the end facet of the waveguide needs to be cleaved and polished, which presents taking advantage of the economies of scale long used by the semiconductor industry. As a result, alignment and packaging accounts for the main cost of the manufacturing of optical components.

Indeed, this is a major inhibitor to technological advancements in the telecommunications industry. In order to fully realize the potential of highly integrated PLCs, a new coupling approach scheme needs to be developed, especially one that permits input and output to a 2-D array of fibers.

1.3 Optical Grating Couplers

An alternative to the previously cited approaches is a grating coupler. Grating couplers offer the ability to couple light from out of the plane of the waveguide into (and out of) a waveguide, thereby permitting optical I/O's to populate literally any area of a PLC rather than being confined to just the edge of a PLC chip. This is a very attractive feature, particularly if the incident and exiting light is at normal incidence(vertical alignment) to the waveguide layer, i.e., fibers are positioned perpendicularly to the surface of waveguides as shown in Fig. 1.1.

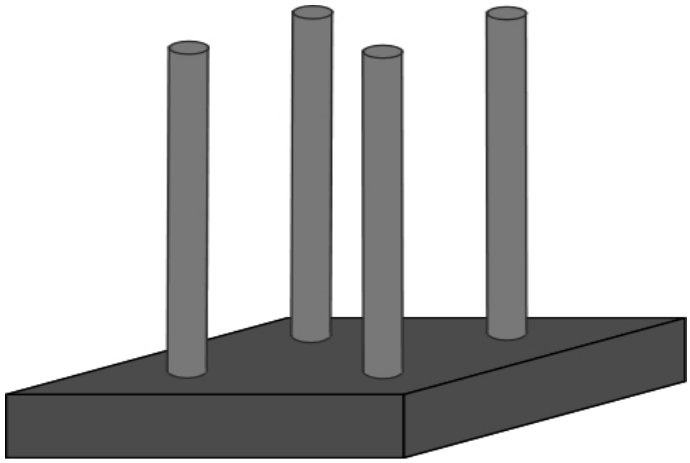

Fig.1.1 Sketch of vertical fiber coupling arrangement.

The vertical fiber coupling approach allows for denser integration because a 2-D array of fibers can be deployed. Also there is no need to cleave and polish the waveguide ends. Thus,

this arrangement results in the possibilities of economies of scale, low manufacturing cost. Depending upon the index contrast, Optical grating couplers propose weak or strong coupling regime. In weak coupling regime, the grating is shallow or the grating refractive index is nearly the same as the cladding. This assures that the effect of grating on the waveguide is small and can be treated as a perturbation. In order to get high efficiency, the grating length has to be rather long. While in strong coupling regime, there is a large refractive index contrast between grating and cladding. Such a grating arrangement is also termed as High Contrast Grating (HCG). HCGs can serve as surface normal broadband, high-reflectivity (>99%) mirrors, which can be used to replace conventional distributed Bragg reflectors (DBRs) in optical devices. Different designs of HCGs can also serve as narrow band, surface emitting, high-quality (Q) factor optical resonators or shallow angle reflectors.

1.4 Silicon-on-Insulator (SOI)

Integrated optical devices are typically based on low refractive index contrast and as a result the relatively large dimension allows only a few functions integrated on a chip. Micro/nano photonic circuits on Silicon-on Insulator (SOI) plays a key role in large-scale photonic integration [3] because of the high refractive index contrast of between Si (3.5) and SiO_2 (1.46). The presence of a silicon-air (high-index contrast) grating on the top silicon layer in SOI allows a strong interaction between the guided mode and the grating. The broadband design of the out-coupler will be presented by optimizing the various grating parameters

1.5 Purpose and outline of work

The purpose of our research is to investigate the use of grating couplers to couple light from nanophotonics waveguides to optical fibers. Focus of the work will be on Silicon-on-Insulator (SOI) high contrast gratings.

In this proposal, design of an out-coupler that exhibits a high coupling strength over a wide wavelength range will be presented. The simulation is done using eigenmode expansion method with the Cavity Modelling Framework (CAMFR) [4] and the results are validated with Finite Difference Method (FDM).

Chapter 2

Optical gratings-Fundamentals & Emerging Trends

Optical grating is a research topic with a long history. It has been comprehensively studied over the years due to its extensive applications in holography, spectroscopy, lasers, and many other optoelectronic devices.

In this Chapter, a general idea of wave guiding theory is given and the waveguide structures that are going to be used in this work are presented.

2.1 Grating coupler theory

In this section the parameters that will take part in the design process to understand the grating coupler are explained.

2.1.1 Bragg diffraction

When the incident light strikes to the surface of a periodic structure, it gets diffracted. The Bragg condition describes the relationship between the incident wave-vectors and diffracted wave-vectors. If there is no grating at the interface between the two materials, the Bragg condition is the same as Snell's Law, which describes refraction at the interface between two materials.

For grating couplers, the Bragg condition can be written as follows, for the first order diffraction:

$$K_{in} \sin\theta + \frac{2\Pi}{\Lambda} = \beta \qquad \text{..... (2.1)}$$

with $\beta = (2\Pi/\lambda_0)\, n_{eff}$ the propagation constant of the guided mode, λ_0 the desired wavelength and n_{eff} the effective index of the fundamental mode, $k_{in} = (2\Pi/\lambda_0) n_{top}$ is the wave vector of the incident wave, n_{top} the refractive index of the background, θ is the incidence angle, and Λ is the grating period[5] .The Bragg condition is only exact for infinite structures. In finite structures there is a finite range of k vectors around the predicted one in which diffraction occurs. Fig. 2.1 shows a simplified representation of the wave diffraction on the surface of the grating.

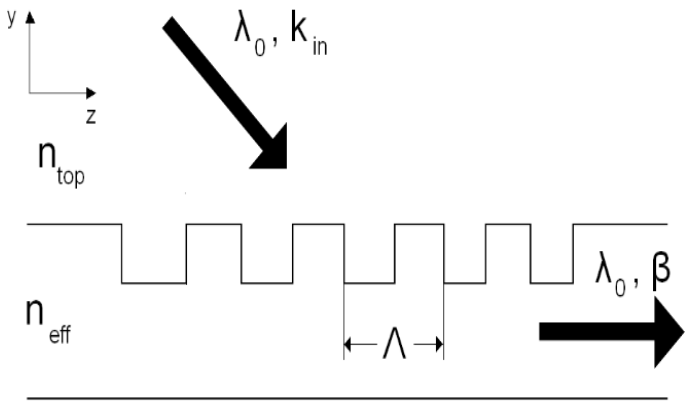

Fig.2.1 Bragg diffraction on the grating surface.

2.1.2 Reciprocity

The scattering matrix, which describes the relations between the inputs and the outputs, comes out to be symmetrical when the materials in a system are reciprocal. The elements of this matrix pursue the following relation [6]:

$$S_{ij} = S_{ji} \quad \text{..... (2.2)}$$

In our case this is very useful, because it means that we can either simulate the coupling from fiber to waveguide or from waveguide to fiber. Since we are using single-mode waveguides and fibers, the coupling efficiency will be the same in both cases.

2.1.3 Symmetry

If the optical fiber is vertically coupled to the grating, as shown in Fig.2.2, half of the power will couple in one direction and the remaining half will be coupled in the other direction due to the symmetry, so the coupling efficiency will always be less than 50%.[6]

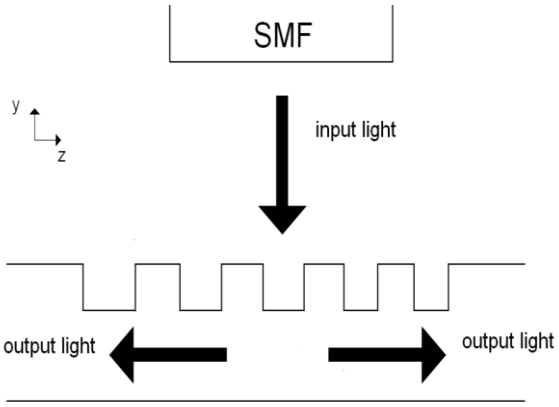

Fig.2.2 Perfect vertical coupling.

Symmetry has to be broken somehow to avoid this issue. This can be achieved by using an asymmetrical grating or by coupling the fiber that is not exactly vertically oriented, but at a certain angle (generally 8^0 to 10^0). In this work both configurations are displayed.

2.1.4 Positive & Negative detuned gratings

The fiber has to be coupled at an angle close to the vertical generally taken nearly in range 8^0 to 10^0 to break the symmetry of perfectly vertical coupling. Such a grating is called detuned grating. These angles can be either positive or negative & the coupling scheme will change for both possibilities of angles, as shown in Fig.2.3. If the angle is positive, the grating is called positively detuned, and if the angle is negative the grating is called negatively detuned.

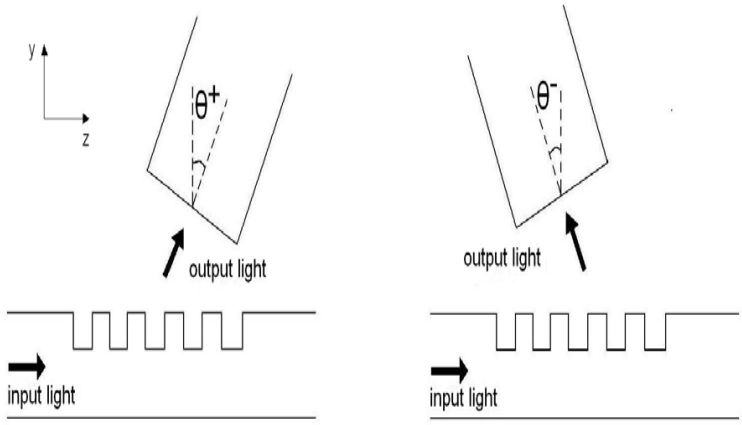

Fig.2.3 Positive and negative detuned gratings.

In a negatively detuned grating, the grating period is smaller or the wavelength is longer compared to the case of vertical coupling. In a positively detuned grating, the grating period is larger or the wavelength is shorter compared to the case of vertical coupling [6].

In this thesis a positively detuned grating will be designed and simulated, because this setup would make the experiments and measurements easier, since this kind of structures are measured by placing a grating coupler at both ends of a waveguide. Positively detuned gratings also have a bigger period, and so its fabrication is easier [6].

2.1.5 Definitions

The grating coupler structure is three-dimensional, but it can be approximated by a 2D structure, because its width is much bigger than the wavelength and the core height. The basic design parameters are shown in Fig. 2.4.

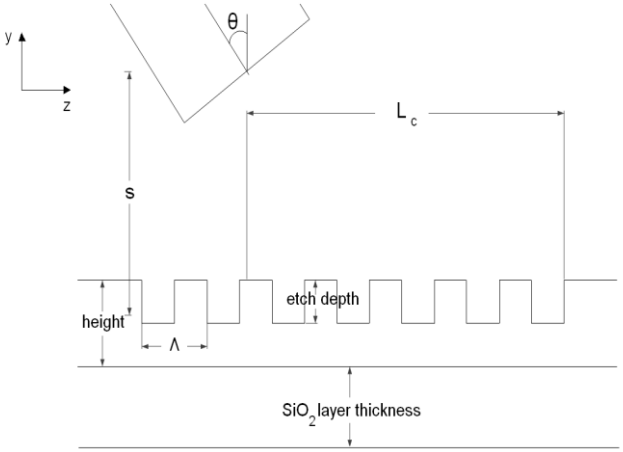

Fig.2.4 Side view of the grating coupler with design parameters.

- Grating thickness (t_g): defined as how much depth with which the guiding silicon layer is etched. Here it is displayed as etch depth.
- Si thickness (t_{si}): the height of the silicon guiding layer. It is displayed in Fig.2.4 as height.
- SiO_2 layer thickness: the thickness of the buried oxide cladding layer.
- θ: angle of the incident field with y-axis (usually ~8º)
- Grating period (Λ): its theoretical value is obtained from (2.1) [6,7,8] :

$$\Lambda_{\text{theory}} = \frac{\lambda_0}{n_{eff} - n_{top}\ \sin\theta} \qquad \text{..... (2.3)}$$

  With n_{eff} the effective index of the guided mode, and n_{top} the refractive index of the top material (normally air or index matching layer).
- Filling factor (C): relation between the widths of the etched sections and the sections without etching.
- Number of periods (N): in our work its value is taken to be 20. It should be enough to make sure the surface of the grating is properly illuminated by the fiber.

2.2 Grating Couplers

An efficient technique for coupling an optical beam onto a thin-film waveguide is to use corrugations in the waveguide. In the case of a surface coupler, we want to couple a guided wave into a radiation mode of the field. While we used coupled mode theory in to describe the effect of a waveguide corrugation, we do not have the luxury of having normalized modes when dealing with radiation modes, so other techniques can be used to determine the effective coupling. In this section, we will describe qualitatively the operation of the coupler.

The grating coupler is shown in Fig.2.5. An incident beam strikes the grating on the waveguide. This grating can be created through lithography, holographic development, or volume index variations through ion implantation, to mention only a few techniques. Here, we are only concerned with the fact that there will be a grating. The incident wave strikes the grating and is broken into several other beams. There is usually a reflected wave, and, if the substrate is transparent, there will be a transmitted beam. The directions of these beams follow Snell's law. There can also be several diffracted waves, where the direction of the beam is dramatically altered from what would be expected through reflection or refraction.

If conditions are correct, a portion of the wave can couple into the guided mode of the waveguide. We will show that the effect of the grating is to modify the longitudinal component of the k vector of the wave.

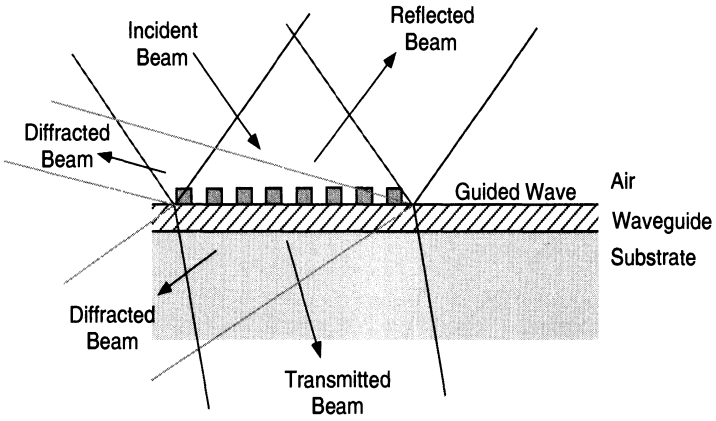

Fig.2.5 The incident beam is broken into transmitted, reflected, and diffracted beams, when a grating coupler is illuminated with an incident beam [9].

2.2.1 Basic Grating Physics

If the grating structure is oriented along the z direction, then it can modify the z (longitudinal) component of the incident wavevector. Specifically, if the grating has a period Λ, the vector relation between incident and diffracted light is

$$K_{out} = K_{in} \pm \frac{2q\Pi}{\Lambda} z \qquad \ldots\ldots\ldots\ldots\ldots (2.4)$$

where q is an integer, subject to the condition that the magnitude of the wavevector does not change

$$|K_{in}| = |K_{out}| \qquad \ldots\ldots\ldots\ldots\ldots (2.5)$$

when the diffracted wave stays in the same index medium. This is most easily viewed graphically. Fig.2.6 shows the input, reflected, and diffracted waves from a surface grating [9]. The period of the waveguide satisfies $K = 2\pi/\Lambda$. The incident wave has a wavevector

$k_0 n_a$, where n_a is the index of the medium above the grating. Upon striking the grating, a reflected and diffracted wave are generated. The reflected wave has the same longitudinal wavevector $k_z = k_0 n_a \sin\theta$, as the input wave, but the transverse component of the wavevector is reversed. The magnitude of the reflected wavevector is identical to the input. The grating can add or subtract integer units of K to the z component of the incident wave. The radius $k_0 n_a$ shows the locus of allowed wavevector values based on Equation 2.5. Any diffracted wavevector must fall on this radius. Graphically,we add or subtract the vector K from the z component of the incident wave, and see where it intersects the radius. In this case, it is impossible to add a vector K and remain on the proscribed radius. Only when K is subtracted from the incident wave is there an allowed solution.

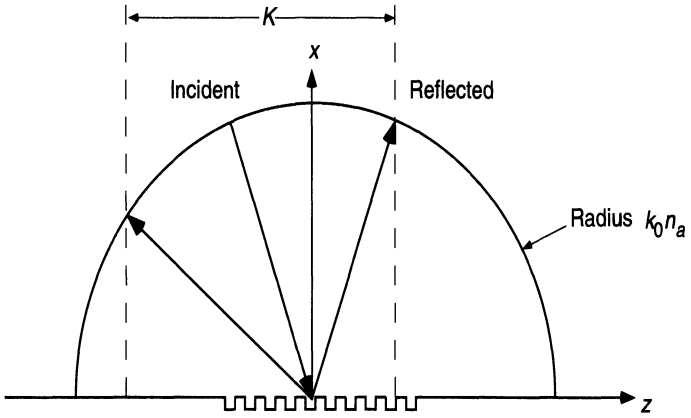

Fig.2.6 K-space diagram of a wave diffracting backwards of a grating, the grating subtracts a value K from the z component of the input wavevector.

Now consider what would happen if the beam is incident on a grating placed in a thin-film waveguide structure sitting on a transparent substrate. The same type of K-space diagram can be drawn, as shown in Fig. 2.7 [9]. In this case, the magnitude of the transmitted wave is larger due to the increased index. The lower radius in the Fig.2.7 represents the allowed values of the diffracted or transmitted wave-vectors in the substrate. The allowed k values of the waveguide are represented by the small section of a radius horizontally located at $k_0 n_f$. In this case, we can see that there can be one beam diffracted backward into the substrate, and one beam diffracted forward into the waveguide.

The horizontal diffracted beam corresponds to the grating scattering a wave into the waveguide, which has an effective wavevector $k_0 n_f$. If the incident angle is θ, then, by geometry, the guided wave propagation coefficient is

$$\beta = k_0 n_a \sin\theta + K \qquad \ldots\ldots\ldots\ldots\ldots (2.6)$$

From these diagrams, we can see how the longitudinal value of the wavevector is converted by the grating into new values. The value k_0 stays the same in all media, but the influence of the dielectric constant n_i is seen to scale the wavevector in each media. However, the effective wavenumber of the grating K, is independent of the index, and simply adds or subtracts to the longitudinal component. If total wavenumber can be preserved after adding in the effect of the grating, then a diffracted order can occur.

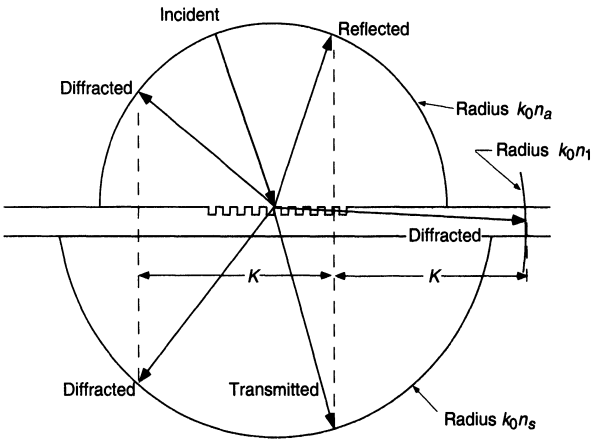

Fig. 2.7 K-space diagram shows a grating on a high-index thin film, placed on a moderate-index substrate. The angle of incidence is exactly right for the grating to couple light into the waveguide.

2.2.2 Output Coupling with a Grating Coupler

The waveguide grating is advantageous because it can be manufactured using lithographic techniques that are standard in the semiconductor industry. This means that it is possible to mass-produce integrated optical devices with waveguide couplers. In this section we want to consider some of the details of such a coupler. Consider the case where a guided mode in a waveguide is incident upon a section of waveguide with a grating. The grating will act as a coupler, and coherently scatter some of the light out of the waveguide. This technique is becoming popular for semiconductor laser output coupling because it is not necessary to cleave the substrate in order to create an output mirror. An example of such a structure is shown in Fig.2.8 [9]. The top of Fig.2.8 shows the waveguide configuration with the incident and transmitted wave, and the diffracted waves going into the substrate and the air.

The incident wave is a guided mode with propagation coefficient β, which by definition is the z component of the wavevector. The grating can add or subtract to this z component. By inspection of Fig.2.8, we can see that it is impossible for a photon to scatter off the grating in a forward direction and have $K_z = \beta + K$. We must consider only cases where the z component is reduced. For the case shown, we see that there are four cases where

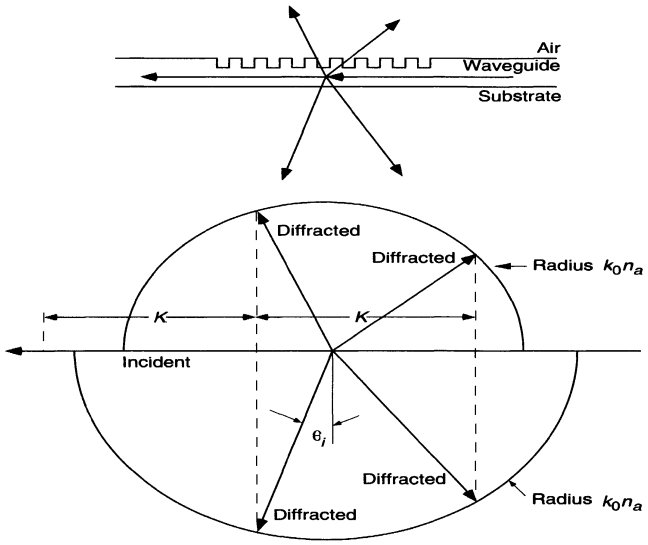

Fig.2.8 Guided wave incident upon a grating will couple some energy into diffracted waves. The angle at which the diffracted beam leaves is determined by the phase-matching conditions shown in the lower diagram.

$k_0 n_i \sin\theta = \beta - qK$ can be satisfied. These are represented by two rays going into the substrate and two into the air. This illustrates one difficulty with grating couplers: they tend to couple light in both directions out of the waveguide. If we were trying to efficiently couple light from a waveguide for an application, we might try to adjust the grating period so that only one beam was coupled into the air. But there would still be a beam coupled into the substrate, which represents a potential power loss of 50 percent.

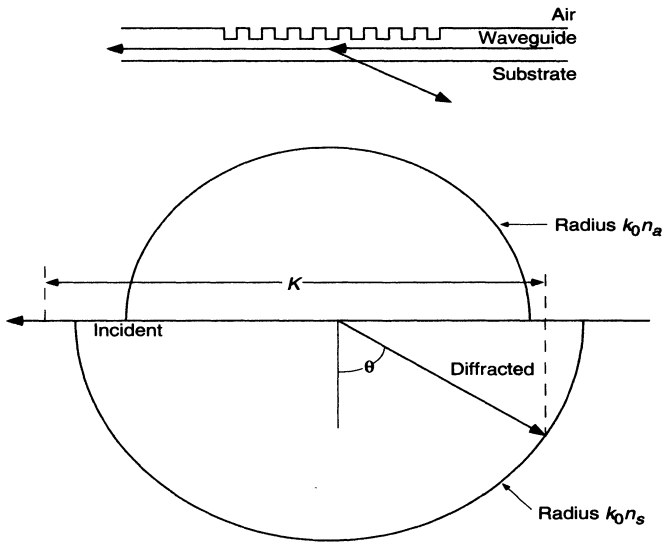

Fig.2.9 Single-beam coupler can be built by making the grating wavenumber so large that the phase-matching condition cannot be met in the cover region. The only coupled power radiates into the substrate.

This can be combated by placing a reflector under the active waveguide, reflecting the power back out of the structure, although one has to be very careful about interference effects between the two coherent waves combining above the waveguide. A second method is to design the grating such that only one beam can couple out of it. If the index of the substrate is greater than the cover index, it is possible to make it impossible for the phase-matching conditions to be realized in the cover region. Fig.2.9 [9] shows the phase diagram of such a structure.

In this case, the grating wavenumber is chosen to almost retroreflect the beam back down the grating. Graphically, we can see that this condition will be met if

$$\beta + k_0 n_s > K > \beta + k_0 n_c$$

Unfortunately, there are several problems with this scheme. First, the exiting beam will strike the lower substrate-air interface above the critical angle, and will not couple into free space. To get light out, it is necessary to deform the lower substrate surface by adding a prism or another grating. This defeats many of the reasons for using gratings in the first place. However, there are situations where it could be useful to couple light out of the waveguide and into other regions of the substrate, such as into a detector. The second problem has to do with the fact that most semiconductors operate in a standing wave. The laser light travels back and forth along the waveguide axis. Using a coupler as shown in Fig. 2.9, two light beams would be coupled out, in nearly opposite directions. This is essentially the same problem as in the air coupling, when the power was divided between two beams.

Another approach to the multiple-beam problem is to use a blazed grating, where the dielectric grating has an asymmetric profile [10]. The effect of the blaze (i.e., the asymmetry) is to cause certain diffraction orders to preferentially receive more of the power. This technique has been used for years in the manufacture of diffraction gratings for scientific instruments such as spectrophotometers and laser tuners.

2.2.3 The Coupling Coefficient

We cannot directly use coupled mode theory to derive the coupling coefficient for a diffraction grating. There have been many calculations of these structures using Green's functions, Bloch waves, and variational techniques. There is currently a great deal of research being done on grating couplers for semiconductor lasers. The grating can serve as both an output coupler and as a combination mirror-tuned filter for providing the necessary optical feedback to sustain laser operation.

2.3 Coupling to fiber

2.3.1 Introduction to coupling

Well-organized coupling between single mode fibers (SMF) and single mode waveguides is a key challenge in silicon photonics. The waveguide is particularly small, with a core cross sectional area of approximately 0.1μm². In comparison an optical fiber has a core with a cross sectional area of around 250 μm² (with a radius of 8-10 μm), three orders of magnitude larger. The size mismatch of single mode waveguides compared with the diameter of a single mode fiber as shown in Fig.2.10 makes the coupling inefficient. So, it is significant to be able to focus the light from a fiber down to the spot size of the waveguide. Traditional approaches used for this challenge are costly and require precise alignment [11]. Fig. 2.10 shows the dimension differences between a SMF fiber and a silicon single mode waveguide.

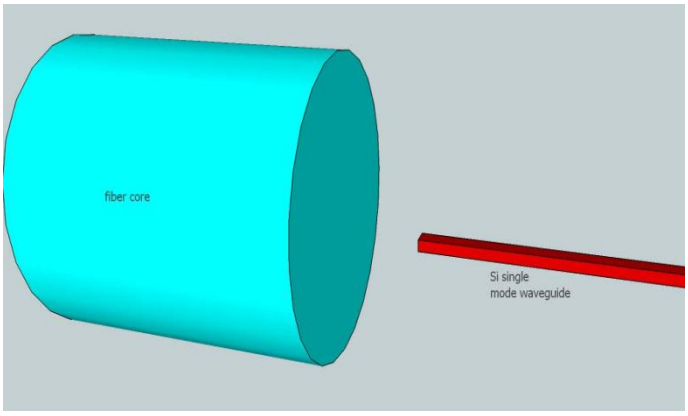

Fig.2.10 Fiber butt coupling to waveguide.

Simple butt coupling between the fiber and the waveguide was traditionally used, but it leads to high coupling losses. There are some approximations to the solution of this problem which have better performance. These solutions are presented in the following section.

2.3.2 Coupling schemes

There are two basic fiber to waveguide coupling schemes: in-plane and out-of-plane couplers. Their coupling schemes and operating characteristics are presented in the following sections.

2.3.2.1 Horizontal coupling using tapered waveguides

Tapers attempt to improve the coupling efficiency by matching the mode dimensions of the field of a SMF fiber with the waveguide dimensions have been suggested here. The required typical taper length must be of the order of millimetres to avoid excessive coupling to

radiation modes in the taper. In addition, these tapers undergo strong back reflections at the surface of the coupler.

Inverse tapers, from the waveguide dimensions to the dimensions of a small tip, have been used significantly for coupling laser diodes to optical fibers. These structures rely on the evanescent field at the tip to increase the mode size of the waveguide to that of the fiber so that proposed structure can acts as an out-of-plane coupler. However, these structures are hundreds of micrometers long [12]. Fig. 2.11 shows the inverse taper and the alignment to the fiber. These kinds of structures present a healthy coupling to fiber.

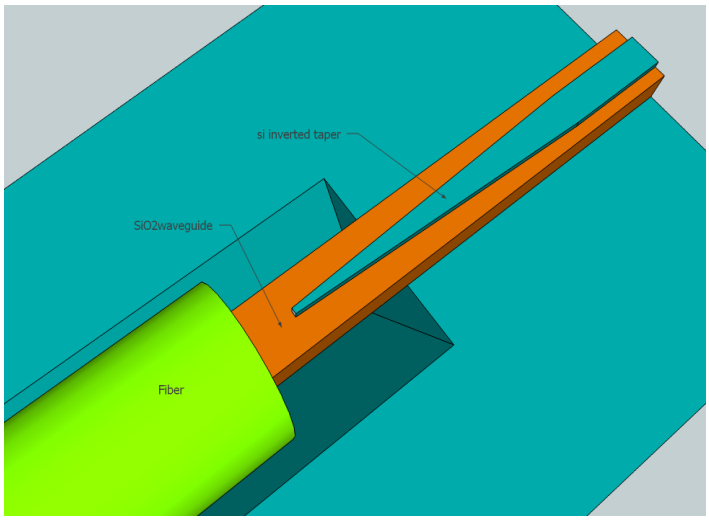

Fig.2.11 Coupling to fiber using an inverse taper [13].

2.3.2.2 Vertical coupling using a grating coupler

An additional solution is to use grating couplers followed by a taper to adjust the lateral size of the incident beam to the sub-micrometer waveguide width. These devices take advantage of the Bragg diffraction phenomenon to couple the light coming from a fiber in case of in-plane coupler. Using the symmetry property described above for grating couplers, same arrangement can also be used for out-of-plane coupler. Several developments of this initial idea have been proposed to reduce the losses, but not all of them are regarded to be fully CMOS compatible. Fig.2.12 shows the coupling scheme to fiber. These kinds of structures are not so robust, but have the advantage that couple light from standard, non-lensed single mode fibers.

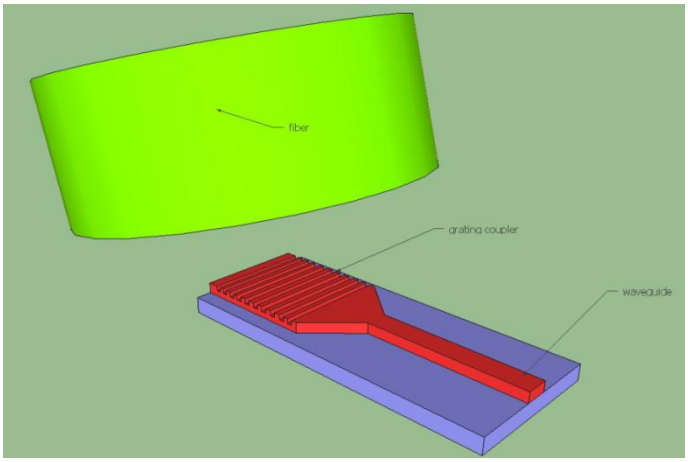

Fig.2.12 Coupling to fiber using a grating coupler.

2.4 SOI Waveguide structures

In this section the structure of an SOI wafer and the possible waveguide structures are exposed. The configuration of an SOI wafer is shown in Fig. 2.13. A silicon dioxide layer is grown under the surface of the silicon wafer. The top layer is then used as the guiding layer.

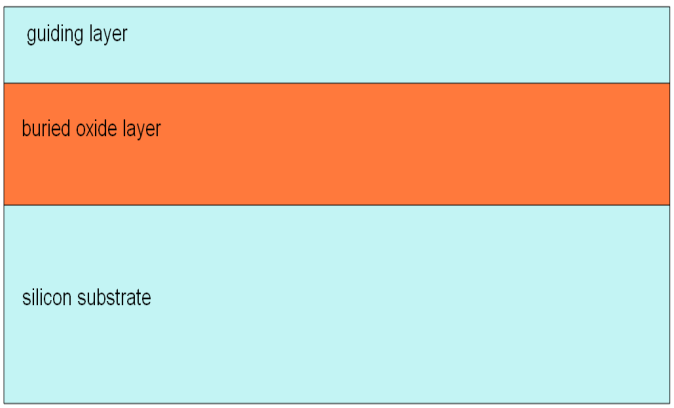

Fig.2.13 SOI wafer structure.

The purpose of the buried oxide layer is to act as the lower index cladding layer, and hence prevent the field associated with the optical modes from penetrating the silicon substrate below. For satisfactory out-coupling, the oxide layer should be thicker than the evanescent fields associated with the modes [14].

The waveguide can be transformed from an asymmetrical waveguide (Fig.2.13, with air on top) to a symmetrical one by the addition of a surface oxide layer at the top of guiding layer. In practice, however, the refractive indices of both air *(n* = 1*)* and silicon dioxide *(n* ~1.5*)* are so different from that of silicon *(n* ~ 3.5*)* that the two configurations are very similar. For many applications, two dimensional confinements may be required. This can be achieved in

silicon by etching a two-dimensional waveguide. There are two main possible structures that can be etched in the silicon layer.

When the dimensions of the core width range from 1 μm to 4 μm, we talk about rib or ridge waveguide structure. The next step is to bring the dimensions of the core width to be in the order of hundreds of nanometres. This is achieved with the so called strip waveguide. Both structures will be explained in more detail in the next section.

2.4.1 Large single mode waveguides

Rib (or ridge) waveguides are composed of a core and two lateral slab regions etched on the silicon layer. The lateral confinement is achieved by means of the leakage of the higher order modes in these lateral slab regions. The cross-section of a rib waveguide is shown in Fig.2.14.

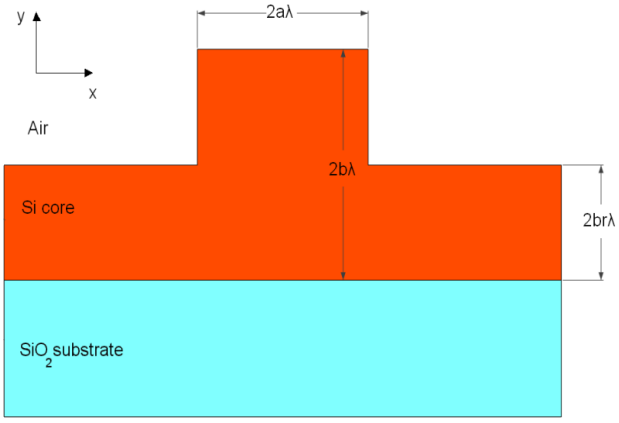

Fig.2.14 Large single mode rib waveguide cross section [15].

2.4.2 Strip nano waveguides

The next step towards miniaturization is bringing the waveguide to dimensions in the order of several nanometres. Recent technological advances make possible this reduction of dimensions. In this case the strip structure is used, in order to achieve higher light confinement. In this case, the core width and height define the single mode region, but the SiO_2 layer width and thickness have to be calculated to obtain good coupling conditions, because the input field is launched in the cladding and then couples to the core.

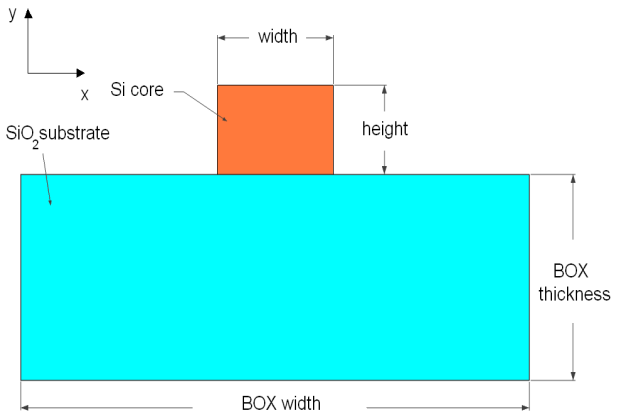

Fig.2.15 Strip nano waveguide cross section.

2.5 Emerging trends in SOI grating coupler structures

Some of recent trends that are being applied to grating coupler structures to boost their performance are reviewed below. They are either one-dimensional or two dimensional solutions [16].

2.5.1 Grating with upper index matching layer

Sometimes, the structure is surrounded by index matching layer at the top of Silicon guiding layer inspite of using air so that fiber facet reflections are minimized, and in this way coupling efficiency is enhanced in vertical direction. The structure is schematically drawn in Fig. 2.16.

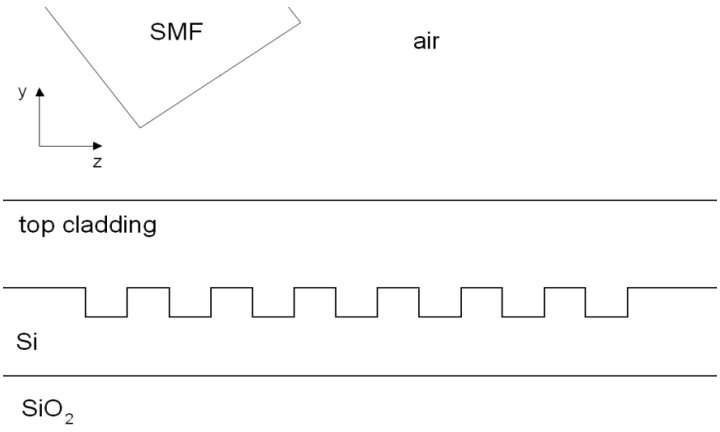

Fig.2.16 Grating coupler with index matching layer.

2.5.2 Grating with bottom reflector

The main restraint to the efficiency of the grating couplers is the leakage to the substrate. A bottom reflector with a multi-layer dielectric mirror or a metal mirror can further improve this ratio and the coupling efficiency to fiber.

It is important to choose the buffer thickness correctly. Depending on which material is used for this bottom mirror, the structure may not be CMOS compatible, and thus not commercially available. Fig.2.17 shows an example of bottom mirror.

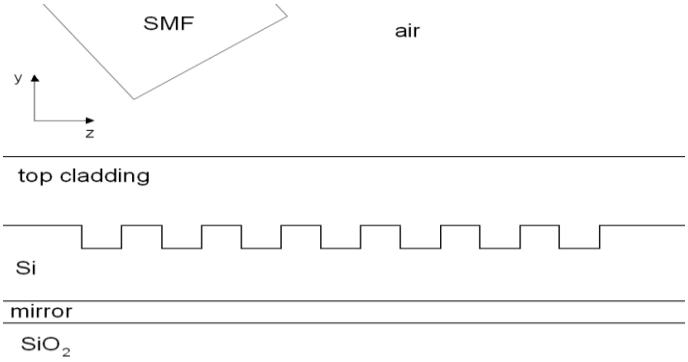

Fig.2.17 Grating coupler with bottom mirror.

2.5.3 Grating with top mirror

The characteristics of a grating coupler can also be changed by adding dielectric layers on top of the grating, in what is called a dielectric stack. The interfaces control the power distribution around the grating ensuring maximal coupling into the guided mode and destructive interference in all unwanted modes. This structure is shown in Fig. 2.18.

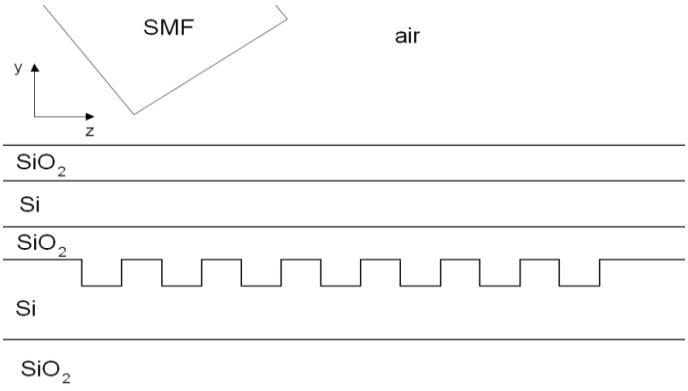

Fig.2.18 Grating coupler with top mirror.

2.5.4 Metal gratings

Metal gratings, fabricated in gold, silver, aluminium or copper, and placed on top of the SOI layer structure can also provide better performances and efficiencies. There is a very high refractive index contrast between the metal teeth and their surroundings. Incredibly high efficiencies are obtained due to the strong scattering on a small length scale. The coupling scheme is shown in Fig. 2.19.

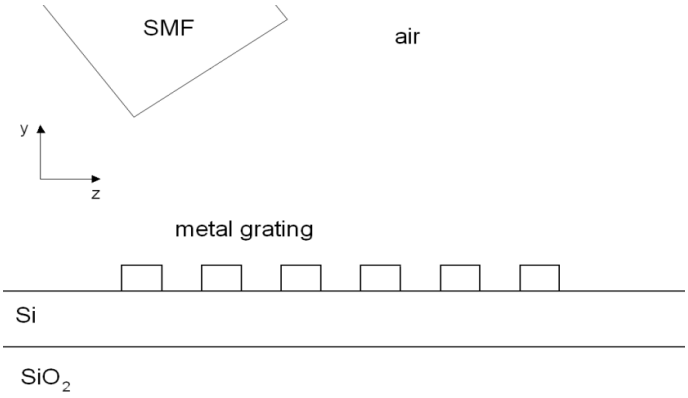

Fig.2.19 Metal grating coupler.

2.5.5 Blazed gratings

An unusual tooth shape (parallelogram or triangular) can be used, in order to suppress the second order reflection or enhance the directionality of the structure. It has been shown that the parallelogram shape is the best shape to achieve the required enhancements. The fabrication of these shapes is although more complicated, because special etch processes have to be performed on them in order to shape the silicon layer. Fig. 2.20 shows this structure.

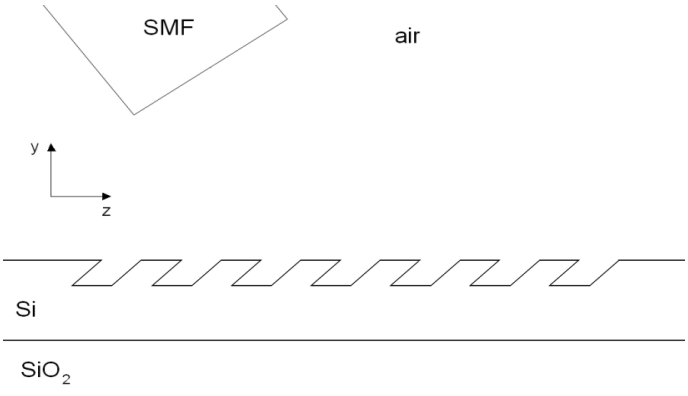

Fig.2.20 Blazed grating coupler.

2.5.6 Chirped gratings

For chirped gratings, the tooth width varies according to some defined relation to minimize back reflection into the waveguide, hence helps in improving coupling efficiency in upward direction. This variation is normally performed only on one part of the structure, while the other is kept unaltered. This variation can be seen in Fig. 2.21.

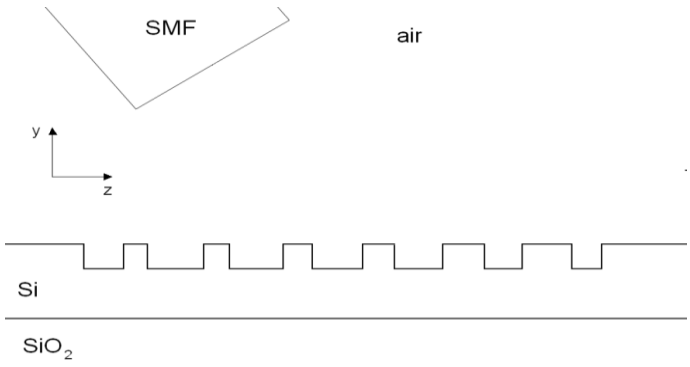

Fig.2.21 Chirped grating coupler.

2.5.7 Gratings with rear reflector

In the case of vertical coupling and a symmetrical structure, the efficiency can never be bigger than 50%, due to the symmetry. A huge amount of power gets transmitted through the length of the waveguide when the arrangement is used as an out-coupler. In order to reduce this transmitted power, a second grating can be introduced next to the first one which will acts as a reflector grating. This grating will reflect almost the entire radiations incident on it as shown in Fig.2.22.

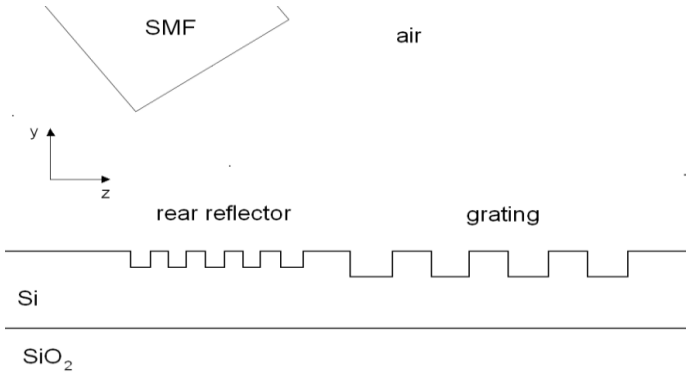

Fig.2.22 Grating coupler with rear reflector.

2.6 Diffraction Grating Applications

2.6.1 Optical Interconnects

As the complexity and speed of integrated circuits and computer systems increase, there is a trade-off between the length of a wire signal path and the bandwidth supported by those paths. Optical interconnects do not exhibit this trade off and in the future will likely replace metal wiring for long interconnects.

Researchers have also shown that optical interconnects provide advantages over electrical interconnects in terms of fan-out, energy conversion, latency, and electromagnetic interference immunity. Several researchers have implemented diffractive grating couplers as the coupling element for optical interconnect systems. Diffraction gratings are desirable because they are more compact than other coupling schemes.

2.6.2 Integrated Optical Devices

Diffraction gratings also find an application in integrated optical devices. Integrated optical devices attempt to accomplish the same task as bulk optics, but on a compact and integrated scale. Some examples of diffractive integrated optical devices are beam expanders, polarisation dependant devices, and holographic filters for beam intensity profile reshaping. Other integrated optical devices with applications to computer systems are optical read/write heads, grating coupled surface emitting lasers, optical sensors, and printer heads.

2.6.3 Fiber Optical Communications

Another area in which diffraction gratings have found application is in fiber optical communications. Optical communications over fiber optic links have potentially large bandwidths and experience low loss for long distances. One advance in the bandwidth of optical communications is wavelength division multiplexing. Wavelength division multiplexing and dense wavelength division multiplexing require devices that are highly sensitive to wavelength for interacting with narrow wavelength communication channels. Diffraction gratings have the potential to play an important role in this arena. Some diffraction grating devices that have been demonstrated by researchers are Bragg gratings for wavelength division multiplexing and optical filters.

2.6.4 Organic light-emitting diodes (OLED's) [17]

OLED's have attracted considerable attention due to their potential for flat panel display application. However, the low light extraction efficiency of OLED's is a serious problem when seeking to realise high brightness and/or long lifetime. In the typical OLED structure, a simple ray optics theory predicts that the percentage of trapped light in the high refractive index of an indium-tin-oxide (ITO) anode and organic layers is as high as 50%.We have confirmed that the total energy of the confined mode is as high as 40-50% by using a more reliable method of combining finite difference time-domain simulation and mode expansion analysis. These results suggest that the most effective method for an improvement of light extraction efficiency is conversion from the confined mode to the output mode in the air.

Chapter 3
Literature Survey

Diffraction grating was discovered by James Gregory (1638-1675), a Scottish mathematician and astronomer, when he observed the diffraction patterns from passing of sunlight through a bird feather. The first man-made diffraction grating was made in 1786 by an American astronomer, David Rittenhouse, who designed a half-inch wide grating by wrapping fine wire around the threads of a pair of fine-pitch screws, with an approximate spacing of about 100 lines per inch [18].

In 1882, at Johns Hopkins University, U.S. physicist Henry Augustus Rowland constructed sophisticated ruling engines, which could fabricate gratings with much higher precision. Rowland published a famous paper [19] in 1882, which opened up a new era of spectral analysis and established grating as the primary optical element of spectroscopic technology.

Today, gratings and other periodic structures have been widely used, not only in spectroscopy, but also in many other areas of science and engineering. Many grating theories and methods have been developed over the years to deal with all kinds of grating problems. Among these theories Rigorous Coupled-Wave Analysis (RCWA) is one of the widely used methods for accurate analysis of the diffraction of electromagnetic waves by periodic structures. Research methodologies developed within the last decade in the field of grating couplers are presented below.

Dirk Taillaert, Wim Bogaerts, Peter Bienstman, et.al. in July 2002 [20] efficiently designed and fabricated an out-of-plane coupler for butt-coupling from fiber to compact planar waveguides. This coupler is based on a short second-order grating or photonic crystal, etched in a waveguide with a low-index oxide cladding. Optimization of coupler is done using mode expansion-based simulations. Simulations using a 2-D model show that up to 74% coupling efficiency between single-mode fiber and a 240-nm-thick GaAs–AlO waveguide is possible. 19% coupling efficiency on test structures have been calculated.

Compact slanted grating couplers to vertically connect fibers and planar waveguides without using any intermediate optics were presented by Bin Wang, Jianhua Jiang, Gregory P. Nordin in 2004 [21]. Strong index modulated slanted grating is employed in the proposed structure.

With the help of a genetic algorithm-based rigorous design tool, a 20μm-long slanted grating couplers (SLGC) with 80.1% input coupling efficiency has been optimized. A rigorous mode analysis reveals that the phase- matching condition and Bragg condition are satisfied simultaneously with respect to the fundamental leaky mode supported by the optimized SLGC.

Dirk Taillaert, Peter Bienstman, and Roel Baets in 2004 [22] have designed a high-efficiency grating coupler for coupling between silicon-on-insulator (SOI) waveguides and optical fibers which works for a broad range of frequencies having grating dimensions of only 13 mm long and 12 mm wide. The size of the grooves is optimized numerically. For TE polarisation the coupling loss to single-mode fiber is observed to be below 1 dB over a 35-nm wavelength range when using SOI with a two-pair bottom reflector.

Nanophotonic waveguides are showing potential for use in the large-scale integration of photonic circuits. In year 2006, Dirk Taillaert, Frederik Van Laere, Melanie Ayre, Wim Bogaerts, Dries Van Thourhout, Peter Bienstman And Roel Baets proposed many different solutions for Coupling light between nanophotonic waveguides and a single-mode fiber [23]. In this paper, a grating coupler approach was discussed such that grating coupler can be easily integrated and placed anywhere on a circuit. They have experimentally demonstrated >30% coupling efficiency with a 1 dB bandwidth of 40 nm on standard wafers. Theoretically, the coupling efficiency can be improved to >90% using an optimized grating design and layer stack. The fabrication of the couplers in silicon-on-insulator and in indium phosphide membranes is also discussed.

Pieter Dumon, Dries Van Thourhout et.al. in 2006 [24] from Ghent University presented compressed wavelength selective functions based on SOI photonic wires, like AWGs, Mach-Zehnder filters and ring resonators, fabricated with CMOS processes. Coupling to single-mode fiber with grating couplers also agree to polarisation-independent performance.

SOI grating structure to obtain perfectly vertical fiber coupling is invented by Gunther Roelkens, Dries Van Thourhout, Roel Baets [25] so that tilting of the fiber is not required to avoid a large second order reflection, thereby reducing the cost of packaging. A grating fiber coupling efficiency of 50% to single mode fiber and 65% to high numerical aperture fiber can

be obtained, with a 3dB bandwidth of 55nm by incorporating a slight asymmetry in the grating structure design. Constraints in the design are related to the manufacturability using 248nm deep UV lithography. The fabrication tolerance of the device is assessed, which is compatible with the state of- the-art Silicon processing techniques.

Frederik Van Laere, Gunther Roelkens, Melanie Ayre, Jonathan Schrauwen, Thomas F. Krauss in January 2007, et.al [26] presented grating couplers fabricated both in silicon-on-insulator (SOI) and InP membranes using BenzoCycloButene wafer bonding for high-efficient coupling between a single-mode fiber and nanophotonic waveguides. Gold bottom mirror is added to to the structures to substantially increase the coupling efficiency. The calculated coupling efficiency to fiber is 69% for SOI grating couplers and 56% for bonded InP membrane grating couplers.

In 2007, Compact Focusing Grating Couplers for Silicon-on-Insulator Integrated Circuits were reported experimentally by Frederik Van Laere, Tom Claes, Jonathan Schrauwen, Stijn Scheerlinck, et.al. [27]. An eight-fold length reduction of the coupling structure from fiber to photonic wire in SOI, as compared to a linear grating and adiabatic taper, is obtained, without reducing the performance capability considerably.

In 2008 [28], interfacing a single mode optical fiber with a nanophotonic silicon-on-insulator waveguide circuit is designed using high efficiency diffractive grating couplers. Silicon overlay was added before grating definition so as to improve the directionality of the diffractive grating structures. 55% coupling efficiency at a wavelength of 1.53μm is experimentally demonstrated on devices fabricated using standard complementary metal oxide semiconductor technology. By optimizing the grating parameters, it was theoretically shown that 80% grating coupling efficiency can be obtained for a uniform grating structure.

Efficiency is enhanced for grating couplers using single mode polymer waveguides through high index coatings [29]. High-index coatings on top of surface gratings strongly improve the grating coupling strength in low-index contrast waveguide systems. New fields of applications for grating couplers such as coupling into single-mode polymer waveguides were opened with this.

High efficiency polarisation splitter based on a one-dimensional grating is experimentally demonstrated with a Bragg reflector underneath by Zhechao Wang, Yongbo Tang, Lech Wosinski, and Sailing He in 2010 [30]. Design, fabrication, and characterization of one-dimensional grating which serve both as a polarisation beam splitter and a vertical coupler for silicon photonic circuits is observed. Bragg reflectors are employed to improve greatly the coupling efficiency. Over 50% efficiency for both polarisations are achieved experimentally, and the extinction ratio between them is also high (-20 dB).

Methods for improving the coupling efficiency of grating couplers for Silicon-on-Insulator Photonic circuits were experimentally demonstrated by Zhechao Wang, Yongbo Tang, Lech Wosinski in September 2010 [31]. A grating coupler-polarisation splitter is measured to have over 50% efficiency for both polarisations. 68% efficiency for single polarisation is achieved by a non-uniform grating coupler.

Yujian Jin, Chenyang Xue, Xiujian Chou, Danfeng Cui, Xiaogang Tong, in 2011 [32] designed a highly efficient grating coupler between optical fiber and Silicon-on-Insulator waveguide. In this paper they presented the design of a diffractive grating structure in order to increase the coupling efficiency between single mode optical fiber and SOI waveguide, and then get the optimal parameters which can reach 67% coupling efficiency. FDTD simulation method was employed for this work. The grating is fabricated on the SOI waveguide by focused ion beam (FIB) lithography. Because side wall roughness caused by fabrication tolerances and extra losses finally we measured a 17.5% coupling efficiency of the grating coupler between optical fiber and silicon waveguide

Work is reviewed on efficient interfaces between a Silicon-on-Insulator photonic IC and a single-mode optical fiber based on grating structures in June 2011[33] by G. Roelkens, D. Vermeulen, S. Selvaraja, student member, IEEE, R. Halir, W. Bogaerts, member, IEEE, and D. Van Thourhout. Several device configurations were presented that provide high efficiency, polarisation insensitivity, and broadband optical coupling on a small footprint. The high alignment tolerance and the fact that the optical fiber interface is out-of-plane provide opportunities for easy packaging and wafer-scale testing of the photonic IC.

A rectangular diffraction grating integrated with a TiO_2 waveguide was modelled by Konrad Ptasinski, Szymon Lis, Marcin Wielichowski and Sergiusz Patela [34]. Design, modelling

and optimizing an optical coupler based on titanium dioxide TiO_2 is described in the following paper. The optimized parameter is the coupling efficiency. Coupler length, grating period, and grating etching depth were also considered as significant parameters. Critical values of grating filling factor preventing the coupling of light into the structure are determined. Finally, parameters of a structure showing the best coupling efficiency are presented.

Enhanced fiber grating coupler integrated by wafer-to-wafer bonding is proposed in June 2011 [35].The ultimate goal of silicon photonics development is the monolithical integration of a photonic layer with optical functions onto silicon IC chips. 3-D stacking is obtained by wafer-to-wafer bonding leading to the photonic layers to be embedded into the last levels of metallization above the IC layer. Method is presented that takes advantage of this integration process in order to realize enhanced fiber grating couplers. Indeed, grating structures are very attractive to couple the light between tiny silicon wires to the external world, which is dominated by optical fibers. Moreover, the insertion of a mirror below the grating is a well-known solution to increase significantly the coupling efficiency.

A novel vertical optical coupler using sub-wavelength High Contrast Grating (HCG) is presented by Li Zhu, Vadim Karagodsky, Weijian Yang, Connie J. Chang-Hasnain in 2011 [36]. Surface-normal incidence plane wave can be coupled into in-plane silicon-on-insulator waveguide with highest efficiency of 84% over a broad wavelength range. Same results can be observed for out-coupler as optical grating exhibit symmetrical property.

Xia Chen and Hon K. Tsang in 2011 [37] proposed an Engineering of Silicon-on-Insulator waveguide gratings for coupling to optical fibers. They have reviewed recent work on waveguide grating couplers. The grating structure may be engineered to enhance the coupling efficiency and bandwidth of grating couplers. Polarisation-independent operation can also be achieved.

Silicon-On-Insulator grating coupler with low back reflection is designed and fabricated to produce an efficient broadband grating coupler on a 400nm thick Silicon-on-Insulator (SOI) wafer [38]. The measured coupling loss is 2.7dB when coupling to a single-mode fiber (SMF) at 1310nm wavelength with TE polarisation. 1dB-full-width and back-reflection are determined to be 30nm and -30dB, respectively.

Chapter 4

Design and Simulation of Broadband SOI Out-coupler

In this section, the structures acting as broadband out-coupler are designed and simulated. As we want to use the grating coupler to couple to optical fibers, we don't only need to calculate how much light is coupled out of the waveguide but also how much couples to the fiber. Here the fiber mode is approximated by a Gaussian profile. This fiber is characterised by its beam diameter.

4.1Design of Grating Out-coupler

4.1.1 Introduction

The basic grating structure is a periodic structure with a finite number of rectangular grating teeth. The grating period for vertical out-of-plane coupling is $\Lambda=\lambda/n_{eff}$. Only in the case of a weak perturbation grating, n_{eff} is the effective index of the unperturbed waveguide mode, otherwise this index must be calculated. Effective index with corresponding Electric field variations for input waveguide of the structure used in Fig.4.2 is shown in Fig.4.1.

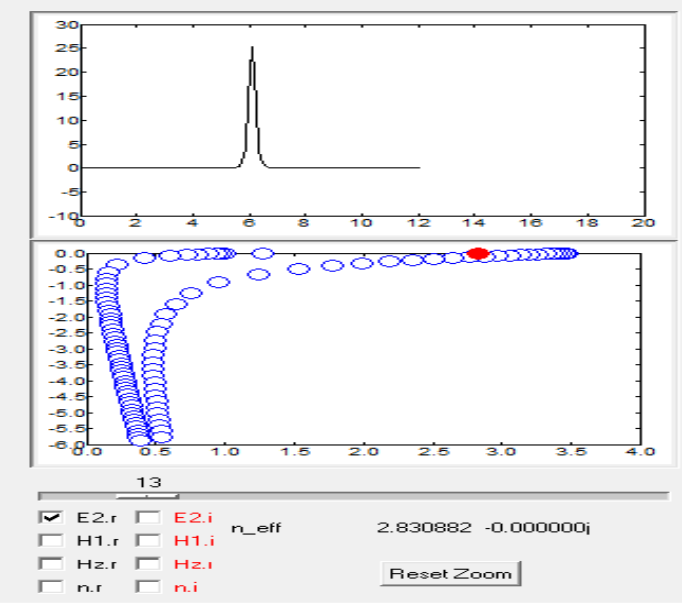

Fig.4.1 Effective index variations along with the corresponding electric field (E_y) variations at guiding mode.

Although several numerical methods and approximate expressions exist to calculate the efficiency of grating couplers, we have used a more general numerical method, the eigenmode expansion method, as it can also be applied to non-periodic structures.

We calculate the coupling efficiency from the waveguide to the fiber. The coupling efficiency from the fiber to the waveguide is the same as to that of waveguide to fiber because the coupling between the two modes (single-mode fiber and waveguide) is considered.

Unfortunately, when light from a grating coupler leaves a waveguide at 90^0, there is also a second-order diffraction which reflects light back into the waveguide. To avoid this unwanted second order reflection, the grating is typically detuned and the light is coupled out at a small angle (generally denoted as θ) with respect to the surface normal direction.

4.1.2 Structure of basic SOI grating out-coupler

The Silicon-on-Insulator (SOI) waveguide consists of a silicon layer on top of a buried silicon di-oxide layer on a silicon substrate. A grating is etched into the silicon core layer in z-direction (called as HCG) and the grating grooves are invariant in the x direction, but the SOI waveguide has a finite width. On top of the silicon there can be air or an index-matching layer (refractive index nearly taken to 1.44). Perfectly matched layers (PML) are embedded on both sides of the structure as PML can absorb radiation travelling toward the walls, without introducing any additional parasitic reflections, regardless of wavelength, incidence angle or polarisation of the incident light. The schematic diagram is shown in Fig.4.2.

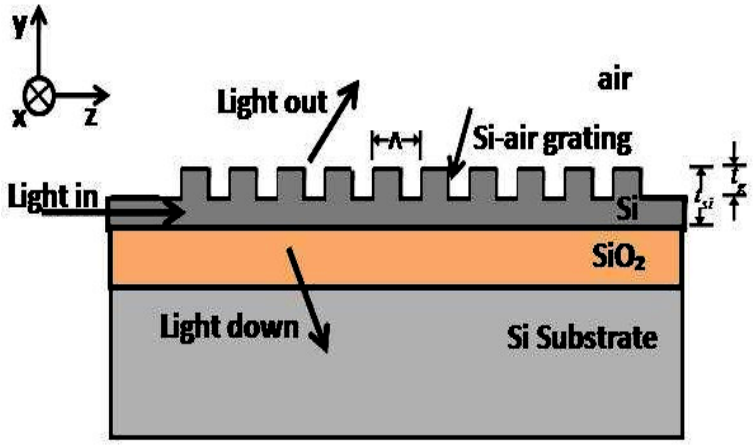

Fig.4.2 Schematic side-view of Out-coupler on SOI with propagation direction z. t_g is grating thickness with Si thickness t_{si}. Λ signifies the period of grating.

Here simulation is done using a uniform rectangular grating of Si-air. Light is input from the left towards the propagating direction z. Light-out is desired to be maximum, so as to maximise the coupling efficiency.

In grating literature, coupling efficiency is often defined as the fraction of the power that is coupled in or out by the grating [39].The thickness of the buried oxide has a major influence

on the coupling efficiency, as described in [40] and [41]. The downward radiated wave partially reflects at the oxide–substrate interface. The oxide thickness should be chosen such that the reflected wave interferes constructively with the directly upward radiated wave. For the used SOI structure, the oxide layer thickness is fixed to 1μm [26].An important part of the power is still radiated into the substrate, since the oxide–substrate interface is not a perfect reflector. This power can be further reduced by introducing multiple bragg mirror in Si-substrate, as bragg reflector reflects almost same power which is incident on it. Hence this reflected power can constructively interfere with the initial power out of the coupler, at required conditions of grating dimensions. Brief concept of bragg mirror reflector is introduced here, detail of which is not needed from our work point. Propagation of the fields using uniform grating is displayed using the field plot as shown in Fig.4.3.

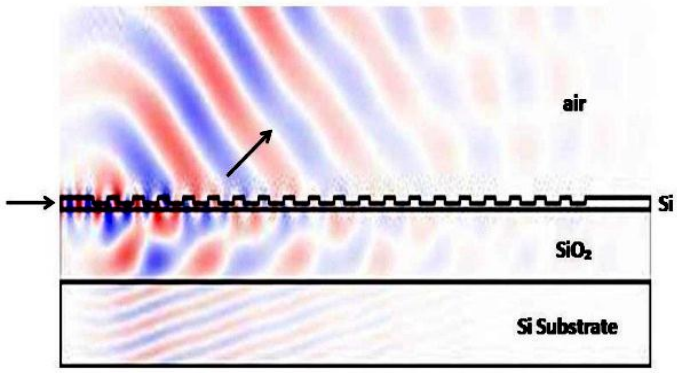

Fig.4.3 Field propagation in Out-coupler.

In the eigenmode expansion method, the coupling to a fiber can be calculated with an Overlap Integral. The coupling to fiber is calculated with the following integral, if we know the electromagnetic fields at the position of the fiber facet [42],

$$\gamma = \frac{\left|\int\int E \times H_{fib}^{*}\right|^{2}}{Re\int\int E \times H^{*}.\ \int\int E_{fib} \times H_{fib}^{*}} \qquad \ldots\ldots\ldots\ldots\ldots (3.1)$$

In above equation, γ describes the overlap between the field and the fiber mode. To calculate the coupling efficiency from a waveguide to fiber, γ must be multiplied by the out-coupled power efficiency. If waveguide mode and fiber mode are normalised, the coupling efficiency to fiber becomes

$$\eta = \left|\int\int_{S} E \times H_{fib}^{*}\, dS\right|^{2} \qquad \ldots\ldots\ldots\ldots\ldots (3.2)$$

,where S is the surface of the fiber.

This formula is exact only in uniform media, but it is accurate here because of the index-matching layer and the fact that a fiber is a weekly guiding structure.

When neglecting the smaller field components, coupling efficiency can be further simplified to

$$\eta = \left| \iint E(x)E(y = y_0, z)A\, e^{-\frac{(x-x_0)^2+(z-z_0)^2}{w_0^2}}\, e^{(jn\frac{2\Pi}{\lambda} z \sin\theta)}\, dx\, dz \right|^2 \quad \ldots\ldots\ldots\ldots\ldots (3.3)$$

, constant A represents the normalization of the Gaussian beam.

θ is the small angle at which the fiber is inclined to surface normal direction of grating to avoid second order reflections. Coupling efficiency depends on this angle θ. Also it is wavelength dependent as shown in above equation. x_0 and z_0 defines the alignment position of the fiber placed above grating in x and z-direction, respectively. If fiber is inclined vertically, i.e. $\theta=0^0$, the whole exponential term will become unity. The end facet of the fiber is kept close to the grating (< 10µm).

4.1.3 Extension with a Gold Bottom Mirror

The coupling efficiency can be increased substantially by using a nearly perfect reflector as a bottom mirror. We have extended the SOI grating coupler with a gold bottom mirror. Before applying the gold mirror, a low-index buffer layer has to cover the grating. We chose BCB (BenzoCycloButene), a low-index (n =1.54 at λ =1.55 µm) polymer with good planarization properties - as the buffer layer. Its thickness is optimized in order to get the constructive interference between the directly upward radiated wave and the reflected wave at the bottom mirror [26]. The optimal simulated BCB buffer thickness is 840 nm, as shown in Fig. 4.4.

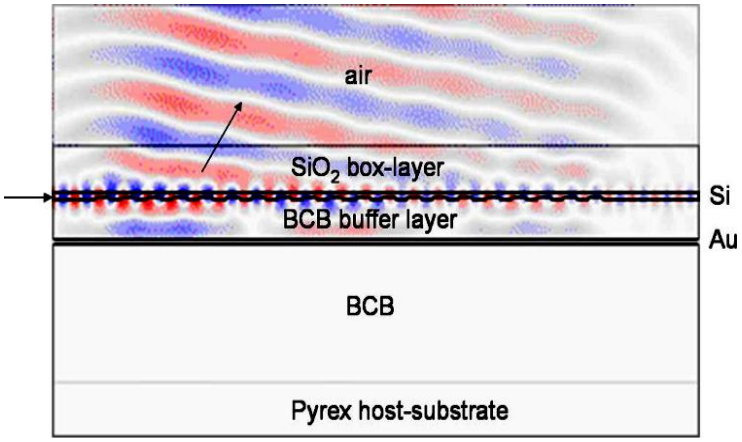

Fig.4.4 Field plot of the optimized SOI structure with a gold bottom mirror.

4.2 Simulation Results

A grating coupler with a uniform grating can have a maximum theoretical coupling efficiency of approximately 80% because the output beam has exponentially decaying power

$$P = P_0 \exp(-2\alpha z)$$

along the propagation direction z, α is called the leakage factor or coupling strength of the grating[22]. It should be noted that above equation is exact only for a long grating with small α, which is not the case for our structure. Therefore we use the results of above equation as a starting point and do a further numerical optimization of the grating structure. We will now discuss in more detail.

4.2.1 Effective refractive index

In homogeneous transparent media, the refractive index *n* can be used to quantify the increase in the wave number (phase change per unit length) caused by the medium: the wave number is n times higher than it would be in vacuum. The effective refractive index n_{eff} has the analogous meaning for light propagation in a waveguide; the propagation constant of the waveguide is the effective index times the vacuum wave number:

$$\beta = n_{eff} \frac{2\Pi}{\lambda} \qquad \text{..... (3.4)}$$

Note that the effective refractive index depends not only on the wavelength but also (for multimode waveguides) on the mode in which the light propagates. For this reason, it is also called modal index. Effective index variations along with Electric field are already shown in Fig.4.1. Obviously, the effective index is not just a material property, but depends on the whole waveguide design.

4.2.2 Coupling efficiency

In grating literature, coupling efficiency is often defined as the fraction of the power that is coupled in or out by the grating. Silicon thickness t_{si}, is the thickness of the guiding Si layer buried over Silicon di-oxide. This Si layer is etched uniformly with rectangular teeth's to form a uniform basic grating structure. Grating thickness t_g, is the thickness of the etched rectangular grating as shown in Fig.4.2

On the basis of the maximum coupling strength that is desired at wavelength 1.55μm for TE-polarisation, the grating thickness (t_g) is chosen looking at the influence of variations in grating thickness (t_g) with grating period (Λ) and Si thickness (t_{si}) as shown Fig.4.5 and Fig.4.6.

For the shallow grating depth, i.e. t_g nearly about 50nm, only a little of power is reflected back at the input of SOI waveguide as desired, but an ample amount of light get transmitted through the propagation direction of waveguide. This transmitted power through the length of SOI waveguide is required to be condensed so that highest coupling strength can be obtained with the fiber placed in upward vertical direction. So t_g should be increased up to 80nm in intervals as shown in Fig.4.5. Increasing the t_g above this value will although reduce the transmitted power, but on the other hand it will increase the reflected power at input of waveguide (muscularly undesirable) and towards the substrate.

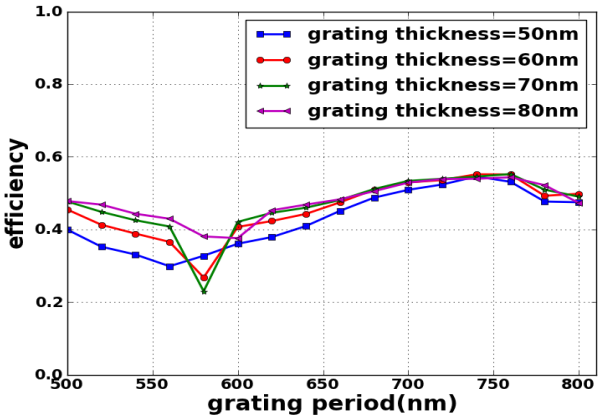

Fig.4.5 Simulation results of coupling efficiency at wavelength, λ=1.55µm for the variations of grating thickness (t_g) with grating period (Λ).

Hence a precise value of t_g should be chosen along with grating period so as to get the significant amount of output power to be coupled with the fiber. At grating period of 500nm, 50% of power is coupled out of the waveguide for t_g=80nm. With the increase in grating period to 600nm, coupling efficiency shows a little dip in efficiency to 38% as seen from Fig.4.5. SOI coupler with grating thickness, t_g=80nm for the various values of periods posses the maximum efficiency of 54% for broad range of grating period, hence it must be chosen.
Also the optimal value of grating period is chosen as 750nm looking at Fig.4.5, as at this grating period, efficient light is coupled out of the waveguide towards fiber. When grating period is around 570nm, ample amount of light is reflected back at the input of waveguide, without being coupled to fiber.

Si thickness t_{si}, also plays a vital role on increasing the outcoupled power. If t_{si} is chosen to be in range less than 200nm, mode overlap between waveguide and fiber will not be good. t_{si} should be near about 220nm,as either increase or decrease in its dimensions reduces the

confinement of power in fiber direction, hence decreases the coupling strength. At lower t_{si} , up to 170nm, less than 25 % of power is coupled to the fiber, and similarly increasing the dimensions of t_{si} over 250nm also don't provide the required maximum coupling strength. For the optimal value of t_g=80nm as selected form Fig.4.5, coupling efficiency of less than 25% is obtained for t_{si} in range from 150nm to 170nm. For t_{si} in range 170nm to 240nm, η shows a steep rise in its strength to nearly 52% from initial strength of less than 25% as can be seen from Fig.4.6. When t_{si} is taken in the range 240nm to 300nm, η will again start decreasing towards the end with minimum value of around 25% at t_{si}=300nm. Therefore an optimal value of t_{si} should be selected which here is taken as 220nm at t_g =80nm & Λ=750nm (reported from Fig.4.5), for λ = 1.55µm as being seen from the Fig.4.6 so that maximum light can be taken out of the plane of waveguide.

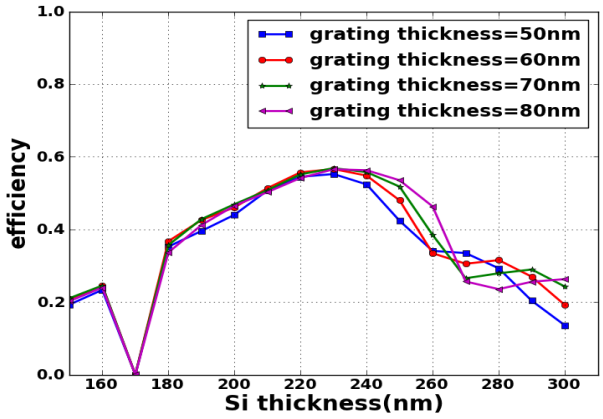

Fig.4.6 Simulation results of coupling efficiency at wavelength, λ=1.55µm for the variations of grating thickness (t_g) with Si thickness (t_{si}).

Duty cycle(C), defined as ratio between the widths of the etched sections and sections without etching, also plays a significant role towards increasing coupling strength. Integrating the results of Fig.4.5 and Fig.4.6, optimized values of t_g=80nm and t_{si}=220nm, maximum coupling efficiency 54% is obtained for various values of duty cycles at Λ=750nm as shown in Fig.4.7.

If the duty cycle is engaged to a large value of 0.7, it will exhibits lower coupling strength of less than 35% at lower values of grating periods in range 540nm to 580nm which is undesirable. Increasing the Λ in the range 600nm to 780nm, η shows an increase from 40% to 55%, respectively for C = 0.7 at λ = 1.55µm. Also lowering the values of duty cycle doesn't show significant change in coupling strength for Λ = 750nm. Hence an optimized value of C = 0.5, must be chosen as justified in the Fig.4.7 to obtain large power for the out-coupler.

As at C = 0.5, maximum coupling efficiency is obtained in comparison to ant other value of duty cycle.

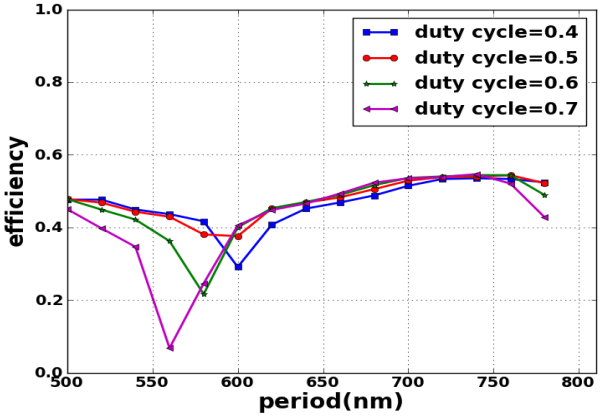

Fig.4.7 Effects of duty cycle(C) on coupling efficiency for various values of Λ with parameters λ=1.55µm, t_g=80nm and t_{si}=220nm.

Integrating the optimized values of t_g & C as seen from Fig.4.5 & Fig.4.7, coupling efficiency is plotted with variations in wavelength from 1500nm to 1650nm in Fig.4.8 for the various values of grating period (Λ) & Si thickness (t_{si}). For lower grating period (Λ=590nm), 20% of coupling efficiency is obtained at λ=1.55µm as displayed in Fig.4.8 (i). Increasing the Λ up to 750nm will provide a significant improvement in coupling strength to 54%. Further increase in Λ above 800nm will again diminish the strength of outcoupled power at λ=1.55µm.

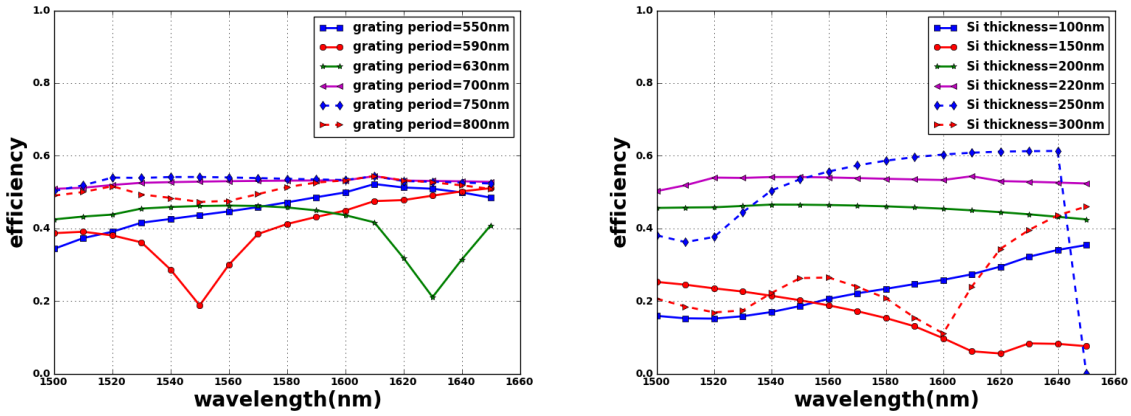

(i) (ii)

Fig.4.8 Coupling Efficiency (η) of a regular grating broadband SOI coupler for variations in grating period (Λ) & Si thickness (t_{si}) with wavelength (λ) at optimized parameters t_g=80nm, C=0.5, t_{si}=220nm.

The proposed structure is acting as a broadband grating coupler displaying a 54% coupling strength for the wide range of wavelengths at grating period (Λ=750nm) shown in Fig.4.8 (i) for the parameters, Si thickness (t_{si} =220nm) , grating thickness (t_g =80nm), and duty cycle (C=0.5). Coupling efficiency variations with wavelength for various values of Silicon thickness (t_{si}) is shown in Fig.4.8 (ii). For lower Silicon thickness (t_{si}=100nm), 20% of coupling efficiency is obtained at λ in range 1500nm to 1550nm as displayed in Fig.4.8 (ii). Increasing the λ up to 1650nm will provide a noteworthy improvement in coupling strength to 36% at λ = 1650nm. Further increase in t_{si} to 220nm will perk up the strength of outcoupled power for the range of wavelength in 1500nm to 1650nm as shown in Fig.4.8 (ii). At t_{si} = 300nm, maximum η of 62% is obtained in λ range 1600nm to 1640nm, but for λ greater than 1640nm, the strength in coupling of light shows a immediate dip, also for λ in range 1500nm to 1580nm, η displays a variations in its strength. Hence t_{si} = 220nm should be chosen so as to obtain a similar coupling efficiency strength of 54% for the whole wavelength range shown in Fig.4.8 (ii).

4.2.3 Coupling efficiency to fiber

As we want to use the grating coupler to couple to optical fibers, we don't only need to calculate how much light is coupled out of the waveguide but also how much couples to the fiber which is defined as the coupling efficiency to fiber. Here the fiber mode is approximated by a Gaussian profile. Fiber can also be aligned at various angles so as to improve the mode overlap between SOI waveguide and optical fiber.

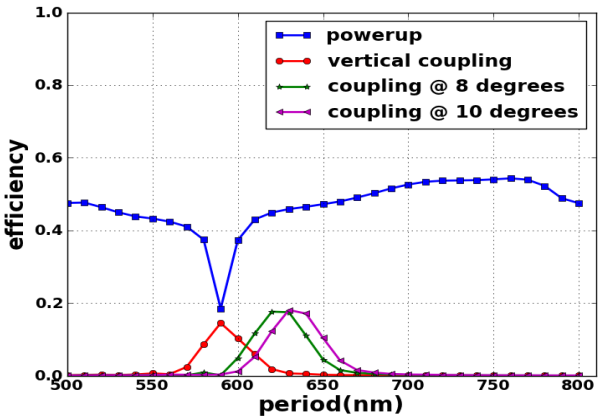

Fig.4.9 Comparison between outcoupled power (powerup) with power coupled to fiber at various angles for TE polarisation at λ=1.55µm with t_{si}=220nm, C=0.5, t_g=80nm.

As can be seen from above Fig.4.9, coupling efficiency to fiber at various angles significantly depends on the period of the grating. Separate values of grating period are required to couple light to fiber placed at different angles.

Vertical efficiency ($\theta = 0^0$) to fiber obtains its maximum value at Λ=590nm, while period for maximum coupling efficiency to fiber placed at 8^0 and 10^0 are 620nm and 630nm, respectively. Powerup here defines that how much power is coupled out of the waveguide, so coupling efficiency to fiber at various angles will always be less than equal to powerup as some of the radiation modes power may get lost. As also can be seen from Fig.4.9 outcoupled power efficiency is always greater than that of vertical coupling power efficiency and coupling efficiency to fiber placed at 8^0 & 10^0.

4.2.3.1 Vertical coupling to fiber

Vertical coupling to fiber is achieved when the angle between fiber axis and y axis is 0^0.

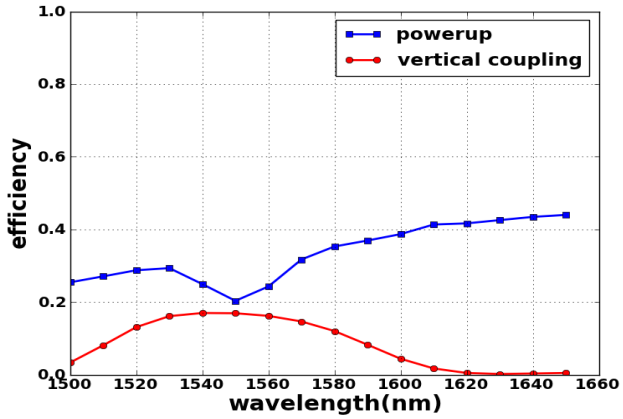

Fig.4.10 Comparison between outcoupled power with power coupled to vertical fiber for TE-polarisation with air on top at Λ=570nm, t_{si}=220nm,C=0.5, t_g=50nm.

For the given set of parameters Λ=570nm, t_{si}=220nm, C=0.5, t_g=50nm,vertical coupling efficiency of 17% can be achieved at wavelength λ=1.55µm, when air is present on the top of grating (Fig.4.10). Although the power coupled out of the grating at the specified set of parameters get reduced, but as the requirement is to couple maximum light to vertically aligned fiber, which is well achieved at this condition. If air is replaced by some index matching layer having refractive index 1.46, degree of power coupled to fiber varies in accordance with the refractive index of the index matching layer (Fig.4.11).

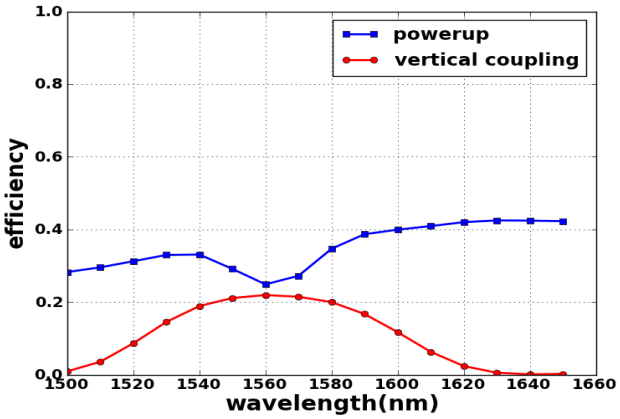

Fig.4.11 Comparison between outcoupled power with power coupled to vertical fiber for TE-polarisation with index matching layer (refractive index=1.46) on top at Λ=570nm, t_{si}=220nm, C=0.5, t_g=50nm.

By using index matching layer of refractive index 1.46 at the top of grating, 4% of improvement can be achieved for vertical coupling with same set of parameters, which can be further improved by using a gold bottom mirror. Vertical alignment of fiber offers less coupling strength in comparison with angled alignment of fiber, but on the other hand its quite easy to align the fiber vertically.

4.2.3.2 Coupling to fiber at different angles

As already seen from Fig.4.9, maximum coupling strength to fiber at different angles vary significantly with period of grating. It is also observed that by using index matching layer at top, outcoupled power strength to fiber for vertical alignment shows an improvement in comparison to air on top.

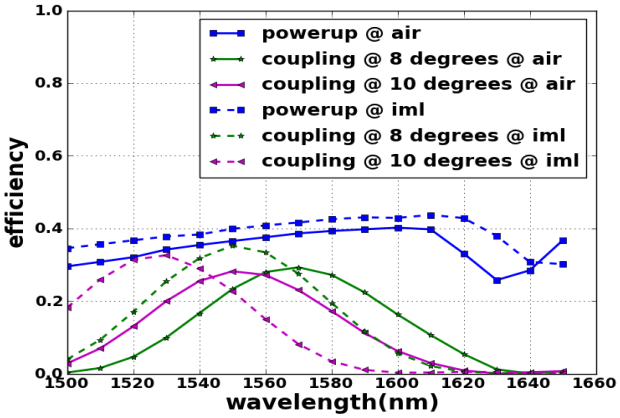

Fig.4.12 Comparison between outcoupled power with power coupled to fiber at different angles of $8^0$and 10^0 for TE-polarisation with air and index matching layer (refractive index=1.46) on top with parameters Λ=610nm, t_{si}=220nm, C=0.5, t_g=50nm, beam diameter of fiber - 12.2µm, alignment of fiber - 7.1 µm.

Variations of coupling efficiency to fiber aligned at $8^0$and 10^0 with air and index matching layer on top for TE polarisation with wavelengths are observed in fig 4.12, for parameters Λ=610nm, t_{si}=220nm, C=0.5, t_g=50nm. Beam diameter of the Gaussian mode fiber and its corresponding alignment with respect to grating also results to variations in coupling efficiency. Here beam diameter is taken as 12.2µm. 23% of power is coupled to fiber at 8^0 with air on top, which gets improved to 35% by using index matching layer (refractive index 1.46) at top for λ=1.55µm. Similarly, 19% of power is coupled to fiber at 10^0 with air on top,which gets improved to 32% by using index matching layer at top for λ=1.53µm. As observing the variations of efficiency with angle of fiber, fiber is aligned at 8^0 with y-axis to gain maximum coupling efficiency. This angled alignment of fiber is also known as detuning of fiber. Power coupled out of the grating at the specified set of parameters get reduced, but as the requirement is to couple maximum light to aligned fiber, which is well achieved at this condition. It is observed that detuning of fiber leads to improvement in power coupling strength in comparison to vertical alignment of fiber.

4.2.4 Coupling efficiency for TE and TM polarisation

A brief idea of coupling efficiency for different polarisations is presented here. Outcoupled power also possesses significant changes in its strength for the variations with different polarisations.

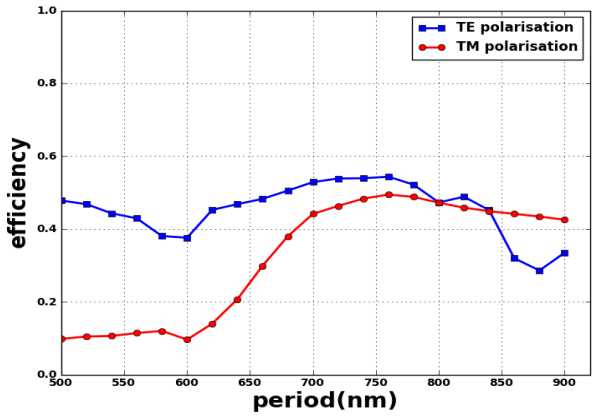

Fig.4.13 Variations of outcoupled power efficiency with period for TE and TM polarisations with air on top at λ=1.55µm, t_g=80nm,C=0.5, t_{si}=220nm.

For the parameters λ=1.55µm, t_g=80nm,C=0.5, t_{si}=220nm,TE polarisation shows a efficient strength in comparison to TM polarisation, which possess a lower value of coupling efficiency. For the lower values of grating periods in range 500nm to 650nm, there is a huge

variation for both polarisations, which get reduced with the increase in grating period. Polarisation insensitivity can be nearly achieved for the larger periods of 800nm-840nm as shown in Fig.4.13. At grating period (Λ) of 800nm, 47% of coupling strength is achieved for both TE & TM polarisations.

Si thickness t_{si}, also plays a fundamental role in obtaining the polarisation insensitive grating coupler. If t_{si} is chosen to be in range less than 200nm, there is a huge difference in efficiency obtained for both TE & TM polarisations as shown in Fig.4.14 (i).

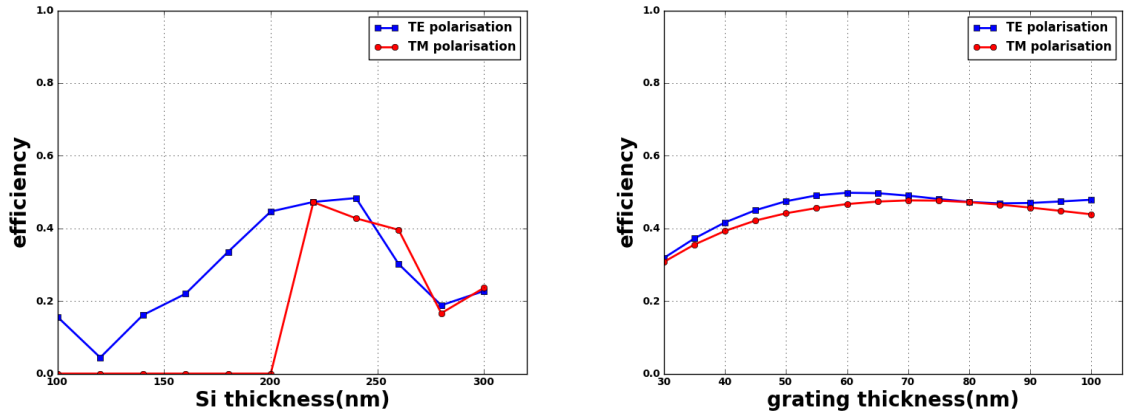

(i) (ii)

Fig.4.14 Coupling Efficiency (η) of a regular grating broadband SOI coupler for variations in (i) Si thickness (t_{si}) & (ii) grating thickness (t_g) for TE & TM polarisations at optimized parameters C = 0.5, Λ = 800nm, λ = 1.55µm.

t_{si} should be taken near about 220nm to obtain polarisation insensitivity, as either increase or decrease in its dimensions reduces the confinement of power in fiber direction, hence decreases the coupling strength. At lower t_{si} , up to 180nm, less than 35 % of power is coupled to the fiber for TE polarisations while for TM polarisation it is almost negligible, and similarly increasing the dimensions of t_{si} over 250nm also don't provide the required maximum coupling strength. Therefore an optimal value of t_{si} should be selected which here is taken as 220nm at C = 0.5 & Λ=750nm (reported from Fig.4.14 (i)), for λ = 1.55µm so that maximum light can be taken out of the plane of waveguide. Integrating the optimal parameters obtained from Fig.4.13 & Fig.4.14 (i), impact of grating thickness to obtain maximum coupled light for different polarisations is shown in Fig.4.14 (ii). It is observed that for t_g in range 30nm to 100nm, almost polarisation insensitive coupler is obtained. But still choice of precise value of t_g is required to be chosen, as it has a significant impact on

increasing the outcoupled power. So t_g = 80nm is chosen, as it provides good coupling strength of 47% for both TE & TM polarisations, hence helps in achieving a polarisation insensitive grating coupler.

Integrating the optimized values of Λ = 800nm, t_g = 80nm, t_{si} = 220nm as seen from Fig.4.13 & Fig.4.14, coupling efficiency is plotted with variations in wavelength from 1500nm to 1650nm in Fig.4.15.

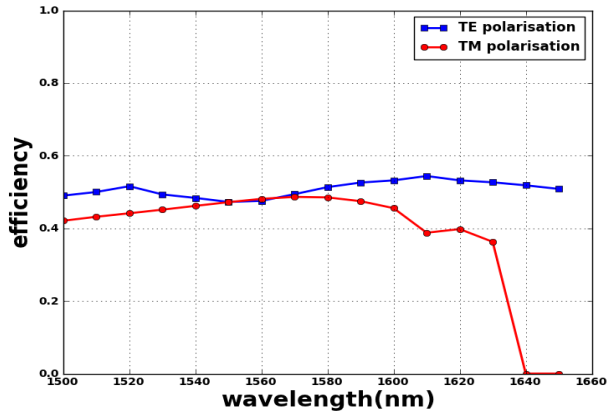

Fig.4.15 Comparison between outcoupled power efficiency with wavelength (λ) for TE & TM polarisation with air on top for optimal parameters Λ=800nm, t_{si}=220nm,C=0.5, t_g=80nm.

For the lower values of λ in range 1500nm to 1530nm, there is approximately 10% difference in strength for both polarisations, which get reduced to almost negligible with the increase in λ to 1550nm. Polarisation insensitivity can be nearly achieved for the 20nm band gap of wavelength, λ from 1550nm to 1570nm as shown in Fig.4.15. For the higher values of λ in range 1580nm to 1650nm, there is again a recognisable difference in strength for both polarisations as can be seen which goes on increasing towards the higher wavelength end.

Hence using the given optimised parameters Λ=800nm, t_{si} =220nm,C=0.5, t_g =80nm, a grating coupler can be proposed which is not polarisation dependent. Coupling efficiency of 47% can be obtained for a band of 20nm ranging from wavelength 1550nm to 1570nm.

Chapter 5

Conclusion

This thesis focuses on the design of compact grating couplers in the strong coupling regime. K-vector diagrams have been explored in order to understand the physical principles of the desired structures. The large index difference between the grating material and the cladding (HCG) strengthens the coupling effect, such that short grating lengths comparable to mode field diameter of a fiber are sufficient for high efficiency coupling. Micro/ nano photonic circuits on Silicon-on-Insulator (SOI) plays a key role in large-scale photonic integration because of the high refractive index contrast of between Si (3.5) and SiO_2 (1.46). In this work, a broadband design of an out-coupler is presented that exhibits a high coupling strength of 54% over a wide wavelength range from 1500nm to1650nm with grating parameters t_g=80nm, C=0.5, t_{si}=220nm, Λ=750nm. Coupling efficiency of 47% is obtained for a grating coupler which is acting as polarisation independent for a 20mm band gap in wavelength range 1550nm to 1570nm at the given optimised parameters Λ=800nm, t_{si}=220nm, C=0.5, t_g=80nm. Further design optimizations of HCG can be applied to realize a narrow-band mirror and/or a high-Q resonator.

The next recommended efforts may focus onto achieving broadband polarisation insensitivity of HCG and its applications in optoelectronics devices, including vertical-cavity surface-emitting lasers (VCSELs), high Q-optical resonators, and hollow-core waveguides.

References

[1] I. Moerman, P. P Van Daele, and P.M. Demeester, "A review on fabrication technologies for the monolithic integration of tapers with III-V semiconductor devices", *IEEE J. Select. Topics Quantum Electron*.3, pp.1308, 1997.

[2] P.V. Studenkov, M.R. Gokhale, and S.R. Forrest, "Efficient coupling in integrated Twin-waveguide lasers using waveguide tapers", *IEEE Photon. Tech. Lett.* 11, pp. 1096, 1999.

[3] W. Bogaerts, R. Baets, P. Dumon, V. Wiaux, S. Beckx, D. Taillaert, B. Luyssaert, J. Van Campenhout, P. Bienstman, and D. VanThourhout, "Nanophotonic waveguides in Silicon-on-insulator fabricated with CMOS technology", *J. Lightwave Technol.*, 23, pp. 401- 412, 2005.

[4] P. Bienstman, CAMFR1.2, Cavity modelling Framework, http://camfr.sourceforge.net. Jun. 2004.

[5] J. V. Galan, P. Sanchis, J. Blasco, and J. Marti, "Study of High Efficiency Grating Couplers for Silicon-Based Horizontal Slot Waveguides", *IEEE Photonics Technology Letters*, vol.20, no. 12, pp.985-987, Jun. 2008.

[6] D. Taillaert, "Grating couplers as Interface between Optical Fibres and Nanophotonic Waveguides", Ghent University, PhD Thesis, Jun. 2004.

[7] Laurent Vivien, Daniel Pascal, Sebastien Lardenois, Delphine Marris-Morini, Eric Cassan, Frédéric Grillot, Suzanne Laval, Jean-Marc Fedeli, and Loubna El Melhaoui, "Light Injection in SOI Microwaveguides Using High-Efficiency Grating Couplers", *Journal Of Lightwave Technology*, vol. 24, no. 10, pp.3810-3815, Oct. 2006.

[8] T. Tsuchizawa, K. Yamada, H. Fukuda, T. Watanabe, J. Takahashi, M. Takahashi, T. Shoji, E. Tamechika, S. Itabashi and H.Morita, "Microphotonics Devices Based on Silicon Microfabrication Technology", *IEEE Journal Of Selected Topics In Quantum Electronics*, vol. 11, no. 1, pp.232-240, Jan./Feb. 2005.

[9] Clifford R. Pollock, Book on "Fundamentals of Optoelectronics", School of Electrical Engineering, Cornell University, 1991.

[10] K.C. Chang and T. Tamir," Simplified approach to Surface-Wave Scattering by Blazed Dielectric Gratings," *Applied Optics* 19, pp.282, 1980.

[11] C. Gunn, "Fully Integrated VLSI CMOS and Photonics", *IEEE Symposium on VLSI Technology 2007*, pp.6-9, Jun. 2007.

[12] V.R. Almeida, R.R. Panepucci, M.Lipson, "Nanotaper for compact mode conversion", *Optics Letters*, vol. 28, no. 15, pp.1302-1304, Aug. 2003.

[13] Zheng Wang, “Design and simulation of spot-size converter for photonic integrated System-in-Package”, TU Berlin, Research Center of Microperipheric Technologies, Master Thesis, 2010.

[14] G.T.Reed and A.P.Khights, “Silicon photonics: an Introduction”, John Wiley & Sons, Ltd, 2004.

[15] R.A. Soref, J. Schmidtchen, and K. Petermann, “Large Single-Mode Rib Waveguides in GeSi-Si and Si-on-SO2”, *IEEE Journal Of Quantum Electronics*, vol. 27, no. 8, pp. 1971-1974, Aug. 1991.

[16] Oriol Gili de Villasante,” Design and Simulation of Vertical Grating Coupler for Photonic Integrated System-in-Package”, Master Thesis, Berlin, Apr. 2010.

[17] M. Fujita, T. Ueno, T. Asano, S. Noda, H. Ohhata, T. Tsuji, H. Nakada and N. Shimoji,” Organic light-emitting diode with ITO/organic photonic Crystal”, *Electron. Lett.*, 39, pp.1750–1752, 2003.

[18] D. Rittenhouse, "Explanation of an optical deception," *Trans. Amer. Phil. Soc.*, vol. 2, pp.37-42, 1786.

[19] H. Rowland, "Preliminary notice of results accomplished on the manufacture and theory of gratings for optical purposes," *Phil. Mag. Suppl*., vol. 13, pp. 469-474, 1882.

[20] Dirk Taillaert, *Member IEEE*, Wim Bogaerts, *Member IEEE*, Peter Bienstman, *Member IEEE*, Thomas F. Krauss, Peter Van Daele, Ingrid Moerman, *Member IEEE*, Steven Verstuyft, Kurt De Mesel, and Roel Baets, *Senior Member, IEEE*,” An Out-of-Plane Grating Coupler for Efficient Butt-Coupling between Compact Planar Waveguides and Single-Mode Fibers”, *IEEE journal of Quantum Electronics,* vol. 38, no. 7, pp.949-955, Jul. 2002.

[21] Bin Wang, Jianhua Jiang, Gregory P. Nordin,” Compact slanted grating couplers”, *Optical Society of America*, vol. 12, no. 15, pp. Optics Express 3313-3326, 26 Jul. 2004.

[22] Dirk Taillaert, Peter Bienstman, and Roel Baets,” Compact efficient broadband grating coupler for silicon-on-insulator waveguides”, O*ptics Letters,* vol. 29, no. 23, pp. 2749-2751, 1 Dec. 2004.

[23] Dirk Taillaert, Frederik VanLaere, Melanie Ayre, Wim Bogaerts, Dries Van Thourhout, Peter Bienstman and Roel Baets,” Grating Couplers for Coupling between Optical Fibers and Nanophotonic Waveguides”, *Japanese Journal of Applied Physics,* vol. 45, no. 8A, pp. 6071–6077, 2006.

[24] Roel Baets, Wim Bogaerts, Dirk Taillaert, Pieter Dumon, Dries Van Thourhout,” SOI Photonic Wire Based Components with Compact and Efficient Fiber Couplers”, *Optical Society of America*, 2006.

[25] Günther Roelkens , Dries Van Thourhout, Roel Baets," SOI grating structure for perfectly vertical fiber coupling", *European Conference on Integrated Optics and Technical Exhibition*, pp. FC4, 2007.

[26] Frederik Van Laere, *Student Member IEEE*, Günther Roelkens, *Student Member IEEE*, Melanie Ayre, Jonathan Schrauwen, *Student Member IEEE*, Dirk Taillaert, *Member IEEE*, Dries Van Thourhout, *Member IEEE*, Thomas F. Krauss, and Roel Baets, *Senior Member IEEE, Member OSA*," Compact and Highly Efficient Grating Couplers Between Optical Fiber and Nanophotonic Waveguides", *Journal of Lightwave Technology*, vol. 25, no. 1, pp.151-156, Jan. 2007.

[27] Frederik Van Laere, *Student Member IEEE*, Tom Claes, Jonathan Schrauwen, *Student Member IEEE*, Stijn Scheerlinck, *Student Member IEEE*, Wim Bogaerts, *Member IEEE*, Dirk Taillaert, *Member IEEE*, Liam O'Faolain, Dries Van Thourhout, *Member IEEE*, and Roel Baets, *Fellow IEEE,"* Compact Focusing Grating Couplers for Silicon-on-Insulator Integrated Circuits", *IEEE Photonics Technology Letters*, vol. 19, no. 23, pp.1919-1921, 1 Dec. 2007.

[28] G. Roelkens, D. Vermeulen, et.al."High efficiency diffraction grating couplers for interfacing a single mode optical fiber with a nano-photonic silicon-on-insulator waveguide circuit", *Applied physics letter* 92, pp.131101 -131101-3 2008.

[29] Roman Bruck and Rainer Hainberger," Efficiency enhancement of grating couplers for single mode polymer waveguides through high index coatings", *Eindhoven, The Netherlands, ThPO7*, pp.201-204, 11-13 Jun. 2008.

[30] Zhechao Wang, Yongbo Tang, Lech Wosinski, and Sailing He," Experimental Demonstration of a High Efficiency Polarisation Splitter Based on a One-Dimensional Grating With a Bragg Reflector Underneath", *IEEE Photonics Technology Letters*, vol. 22, no. 21, pp.1568-1570, 1 Nov. 2010.

[31] Zhechao Wang, Yongbo Tang, Lech Wosinski," High Efficiency Grating Couplers for Silicon-on-Insulator Photonic Circuits", *ECOC 2010*, Torino, Italy, pp.P2.06, 19-23 Sep. 2010.

[32] Yujian Jin, Chenyang Xue, Xiujian Chou, Danfeng Cui, Xiaogang Tong," Highly Efficient Grating Coupler between Optical Fiber and Silicon-on-Insulator Waveguide", *International Conference on Electronics and Optoelectronics (ICEOE 2011)*, pp.V2-382 – V2-384, 2011.

[33] G. Roelkens, D. Vermeulen, S. Selvaraja, Student Member, IEEE, R. Halir, W. Bogaerts, Member, IEEE, and D. Van Thourhout," Grating-Based Optical Fiber

Interfaces for Silicon-on-Insulator Photonic Integrated Circuits", *IEEE Journal Of Selected Topics In Quantum Electronics*, vol. 17, no. 3, pp.571-580, May/ Jun. 2011.

[34] Konrad Ptasinski, Szymon Lis, Marcin Wielichowski and Sergiusz Patela, "Modelling and optimization of grating coupler for slab waveguide", *International Students and Young Scientists Workshop "Photonics and Microsystems"*, pp.66-68, 2010.

[35] Christophe Kopp, Emmanuel Augendre, Regis Orobtchouk, Olivier Lemonnier, and Jean-Marc Fedeli," Enhanced Fiber Grating Coupler Integrated by Wafer-to-Wafer Bonding", *Journal Of Lightwave Technology*, vol. 29, no. 12, pp.1847-1851, 15 Jun. 2011.

[36] Li Zhu, Vadim Karagodsky, Weijian Yang, Connie J. Chang-Hasnain, "Novel High Efficiency Vertical Optical Coupler Using Subwavelength High Contrast Grating", *OSA/ CLEO*, pp.JTu12.pdf, 2011.

[37] Xia Chen and Hon K. Tsang," Engineering of Silicon-on-Insulator Waveguide Gratings for Coupling to Optical Fibers", *The 16th Opto-Electronics and Communications Conference, OECC 2011*, Kaohsiung, Taiwan, pp.845-847, 4-8 Jul. 2011.

[38] Neil Na, Harel Frish, I-Wei Hsieh, Oshrit Harel, Roshan George, Assia Barkai, and Haisheng Rong, "Silicon-On-Insulator Grating Coupler with Low Back-Reflection", *IEEE*,WC5, pp. 54-55, 2011.

[39] T. W. Ang, G. T. Reed, A. Vonsovici, A. G. R. Evans, P. R. Routley, and M. R. Josey, "Effects of grating heights on highly efficient unibond SOI waveguide grating couplers," *IEEE Photon. Technol. Lett.*, vol. 12, pp.59–61, Jan. 2000.

[40] R.M. Emmons and D. G. Hall, "Buried-oxide silicon-on-insulator structures Wave-guide grating couplers", *IEEE J. Quantum Electron*, 28, pp.164–175, Jan. 1992.

[41] T. Suhara and H. Nishihara, "Integrated-optics components and devices using periodic structures", *IEEE J. Quantum Electron*, vol. QE-22, 6, pp.845–867, Jun. 1986.

[42] E.G. Neumann," Single-mode fibers - fundamentals", *Springer-Verlag, Berlin*, 1988.